Provenance Studies of a Set of Pick-Up Glass Fragments Found in Portugal and Dated to the 17th Century

Francisca Pulido Valente, Inês Coutinho, Teresa Medici, Bernard Gratuze, Luís Alves, Ana Cadena, Márcia Vilarigues

heritage

MDPI

Article

Provenance Studies of a Set of Pick-Up Glass Fragments Found in Portugal and Dated to the 17th Century

Francisca Pulido Valente [1,2,*], Inês Coutinho [1,2], Teresa Medici [2], Bernard Gratuze [3], Luís C. Alves [4], Ana Cadena [1,2,3] and Márcia Vilarigues [1,2]

1 Department of Conservation and Restoration, NOVA School of Sciences and Technology, Campus de Caparica, 2829-516 Caparica, Portugal; icoutinho@fct.unl.pt (I.C.); a.irizar@campus.fct.unl.pt (A.C.); mgv@fct.unl.pt (M.V.)
2 Research Unit VICARTE-"Vidro e Cerâmica para as Artes", Campus Caparica, 2829-516 Caparica, Portugal; teresa.medici2@gmail.com
3 RAMAT—Centre Ernest-Babelon, CNRS Université d'Orléans, 3D rue de la Ferollerie, 45071 Orléans, France; bernard.gratuze@cnrs-orleans.fr
4 Centro de Ciências e Tecnologias Nucleares (C2TN), Instituto Superior Técnico, Universidade de Lisboa, 2695-066 Bobadela LRS, Portugal; lcalves@ctn.tecnico.ulisboa.pt
* Correspondence: franciscapulidov@gmail.com

Abstract: One of the most recognized decorations of the *pick-up* technique is the *millefiori* glass, which has been commonly attributed to Venetian production. However, Portugal is the country where the largest known assemblage of this type of glass artefact has been studied and published. In this work, two important archeological contexts were selected: (1) Santa Clara-a-Velha monastery (SCV) and (2) São João de Tarouca monastery (SJT). The fragments selection was made based on the diversity of decorative motifs, colors, and original forms that has been associated with Portuguese production. The compositional characterization was conducted by performing micro-particle-induced X-ray emission (μ-PIXE) mapping, which facilitated the visualization of the distribution of different oxides across the different glass layers and laser ablation inductively coupled plasma mass spectrometry (LA-ICP-MS) to obtain the major, minor, and trace elements composition, including rare earth elements (REEs) to determine which kind of raw materials were used. Additionally, μ-Raman spectroscopy was employed to investigate the opacifiers, while UV–Visible spectroscopy was used to study which chromophores are presented in the glass samples. All the analyzed glass layers can be considered to be of a soda–lime–silica type, and four different geological patterns (from GP1 to GP4) were detected and reported. This result can indicate that these objects were made by using silica sources taken from four different geological settings. Interestingly, the GP3 represents about 41% of the analyzed glass fragments and is compatible with the pattern detected in some production wastes found in two different archeological contexts located in Lisbon, which reinforces the veracity of the theory that this GP can be attributed to a Portuguese production. On the other hand, GP1 was probably attributed Granada provenance.

Keywords: *millefiori* glass; Renaissance; archeology; archeometry; Venetian and *Façon-de-Venise* glass; glass in Portugal

Citation: Valente, F.P.; Coutinho, I.; Medici, T.; Gratuze, B.; Alves, L.C.; Cadena, A.; Vilarigues, M. Provenance Studies of a Set of Pick-Up Glass Fragments Found in Portugal and Dated to the 17th Century. *Heritage* **2024**, *7*, 5048–5083. https://doi.org/10.3390/heritage7090239

Academic Editors: Sara Fiorentino and Tania Chinni

Received: 22 July 2024
Revised: 30 August 2024
Accepted: 9 September 2024
Published: 12 September 2024

1. Introduction

The *pick-up* technique has two different groups of patterns: *millefiori* and *splashed*. The difference between both is that, while the *splashed* pattern uses small, colorful shards of glass to decorate the glass surface of the object, giving it a speckled appearance, the *millefiori* pattern uses *murrine* (sliced canes that have colorful geometrics and concentric patterns observed on its cross-section) appearing to have been decorated with small glass flowers [1].

These objects are extremely rare, and *millefiori* patterns have been considered in the literature as "a perfect type of glass" [2], "one of the most magnificent Venetian glass" [3,4], and have been viewed as a work of art and, simultaneously, as a way to control, imitate, and even surpass nature through alchemy and expert skills [5,6].

Surprisingly, Portugal is the country where the largest known assemblage of archeological *pick-up* glass fragments has been studied and published, and, in the past, a great part of them has been attributed to a Venetian provenance due to the high level of complexity involved in this technique [1]. Venetian glass enjoyed significant popularity in Portugal, and numerous documents attest to its importation and widespread diffusion among the wealthiest members of Portuguese society. It was so appreciated that during the reign of the Portuguese King D. Manuel I (from 1495 to 1521), only he had the exclusive privilege of selling Venetian glass in Portugal [7].

Yet, that seems to have changed between the 16th and 17th century. Some historical documents attest that Portugal was also producing glass in several different regions between the 16th and the 17th centuries (Figure 1), and some of them are documented to have a quality comparable to the Venetian glass objects, also known as *façon-de-Venise* [7–9]. This was not strange, as some archeometric investigations proved that *pick-up* glass was being produced in other countries outside Venice: Spain [10], The Netherlands [11–14], and England [15].

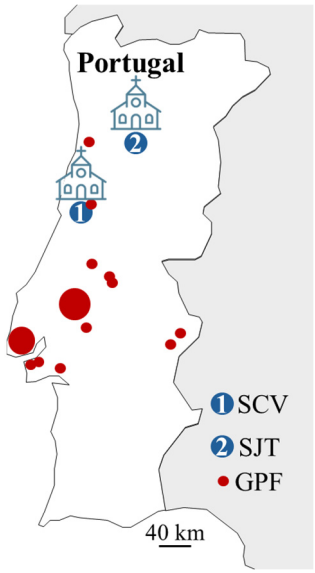

Figure 1. Map of Portugal, with the glass production furnaces dating to the 16th and 17th centuries and the considered archeological contexts signed [8]. The largest of the red circles indicates that in that region of the map, more than one glass production furnace was reported in the consulted literature.

In a royal letter, dated to 15 July 1563, Cardinal D. Henrique (principal regent of Portugal while the legitimate successor to the throne was too young to reign) forbids the import and sale of Venetian glass in the country arguing that, there is in Portugal, a glass of comparable quality and noting that this was a protective measure for Portuguese glassmakers [16].

However, one year earlier (April of 1562), a royal charter forbade the settlement of glass furnaces and the destruction of the existing ones at less than "7 léguas" (almost 34 km) from Lisbon due to the excessive consumption of wood and its consequent price rising and lack of fuel for the daily life of its population [16].

As suggested by José Pedro Barosa, this seemingly contradictory information may be considered as a sign of political pressure due to some Portuguese conflicts with Venice, as Venice was causing problems in the Adriatic Sea for the trade of oriental spices made by Portuguese merchants, and the restriction was directed exclusively to Venetian glass and not to glass

imports from other high-quality production centers such as Antwerp [16]. All this information can be viewed as written evidence to support the existence of Portuguese production.

Unfortunately, there is a gap in the material record of furnaces and objects of known Portuguese origin, which has greatly hindered the study of Portuguese glass production in this period [7]. Having this in mind, archeometrical studies have been developed to better understand what was being produced in Portugal, what was being imported, and from where.

Considering the results of studies performed on archeological glass found in Portugal and dated to the Modern period we can highlight that (1) some objects, like the gourd-shaped vessel, frequently appear exclusively in Portugal [17]; (2) focusing on *millefiori* glass, new decorative patterns, like the cross of Christ and Caravel, appear in fragments found in Lisbon [18]; (3) new colors applied in the glass body [19] and (4) the very high alumina values (Al_2O_3 > 6 wt%) measured for glass found in Portugal are not comparable with any known European glass production center [20,21]; and (4) the geochemical pattern of glass slags found in Lisbon are compatible with the *millefiori* glass fragments also found in the capital [18].

Interestingly, in previous studies performed by Augusta Lima and co-authors [20] and Coutinho et al. [21] of *pick-up* glass from the Santa Clara-a-Velha monastery (Coimbra), genuine Venetian attribution was possible for a few glass fragments and some *filigrana* glass found in Largo do Chafariz de Dentro (Lisboa) [22]. The *millefiori* glass fragments, found in the Santa Clara-a-Velha monastery (SCV), have a high amount of Al_2O_3 (3–6 wt%), which may be compatible with Tuscany production [20].

Although these new observations allow for better understanding Portuguese glass-making technology, we propose that by studying fragments produced by the *pick-up* technique, and combining morphological characteristics (form, decorative motifs, and range of colors) with compositional studies, it will be possible to build patterns that will allow us to identify possible Portuguese provenance. We hope that, in the future, this method can help to distinguish productions without the necessity of carrying out expensive and time-consuming analyses.

Archeological Context and Material

Two archeological contexts were chosen based on different aspects:

- Santa Clara-a-Velha monastery (SCV), is known to be the archeological site with the largest assemblage of *millefiori* glass fragments ever found around the world [1] (Supplementary Material). Here, new decorative patterns, glass colors, and shapes were observed [19].

This monastery is one of the most important Portuguese religious sites because it was where the only Portuguese Queen to be declared a saint by the Catholic Church (The Holy Queen Elisabeth of Portugal, 1271–1336) wanted to be entombed. For this reason, this monastery became an important place of pilgrimage and was inhabited by nuns of noble families and upper bourgeoisies, who probably brought their personal objects/ornaments with them [23]. Here, is important to note that, at that time, it seems like becoming a nun was more related with social status/protection than with personal devotion, and this observation may contribute to justifying the great number of luxurious items that were found in this context, where nuns that followed the vows of poverty, chastity, enclosure, and obedience lived [24].

The SCV monastery was occupied by the Poor Clares Order from the 13th century to 1677, when a new location had to be chosen due to frequent flooding. Most of glass artifacts are dated to the first half of the 17th century, coinciding with the period of the Queen's canonization (25 May 1625) by Pope Urban VIII [23].

The total number or *pick-up* glass objects found in this context was 34 (29 *millefiori* and 5 splash). They were previously morphologically characterized by T. Medici [7], and 19 fragments were also chemically characterized by A. Lima [20]. For this study, 21 glass fragments were selected to be analyzed for the first time. This selection includes two fragmented

murrine canes (SCV_364 and SCV_366); one base of a small bottle (SCV_369); three small bottlenecks, one of them being made in a gourd shape (SCV_046); and the other fragments belong to unknown parts of undetermined objects (Figure 2).

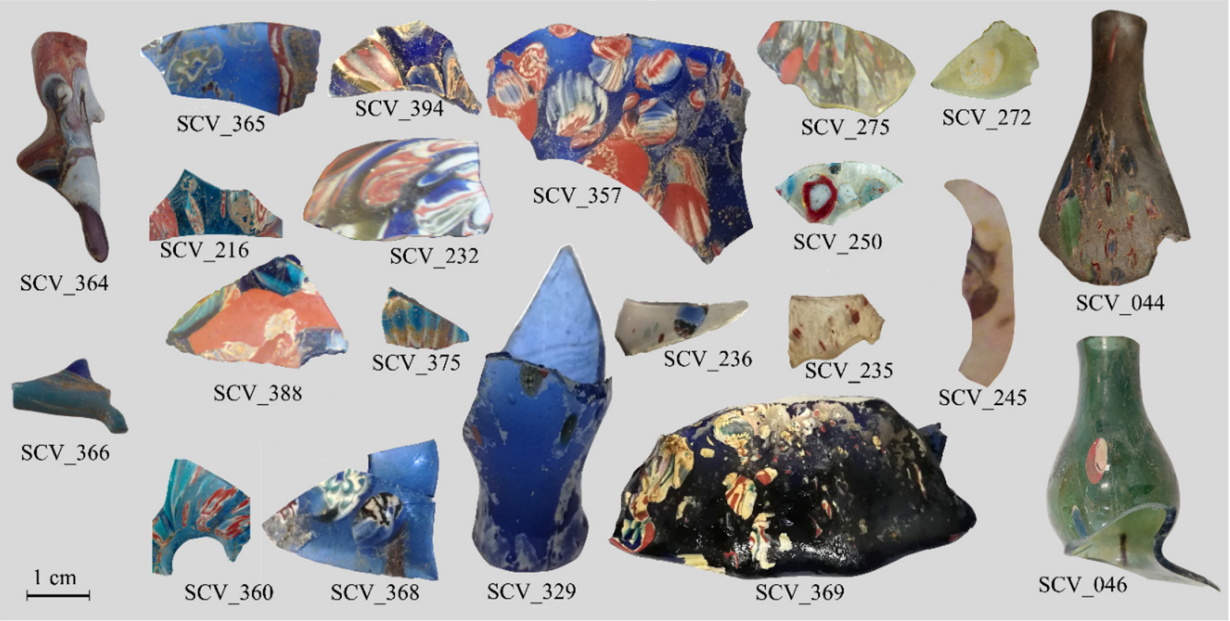

Figure 2. Selected pick-up glass fragments found in Santa Clara-a-Velha monastery to be analyzed.

- São João de Tarouca monastery (SJT) was selected because a small, fragmented *millefiori* flask decorated with the particular "cross of Christ" pattern and a small fragment belonging to a rim and part of the wall of a blue glass vessel decorated with *rosette* pattern (Figure 3) were found here.
  The SJT site is the oldest Portuguese Cistercian monastery, and it was classified as a National Monument in 1956 [25]. It is connected to the French Clairvaux monastery, with its first documentation dating back to 1144 [26]. The connection with glass working of the Cistercian Order are reported in some documents that mentioned that they were able to make small objects like paternosters and "pilgrimage hardware" [27]. These fragments were dated to the 17th century, and the symbol of the *cross of Christ* was adopted by the Military Order of Our Lord Jesus Christ, which inherited, in Portugal, all the heritage that belonged to the Templar Order [28]. This cross, also known as the Portuguese cross, is an important symbol for Portuguese identity, being used on contemporary coins, in the caravel sails, and architectural ornaments [29].

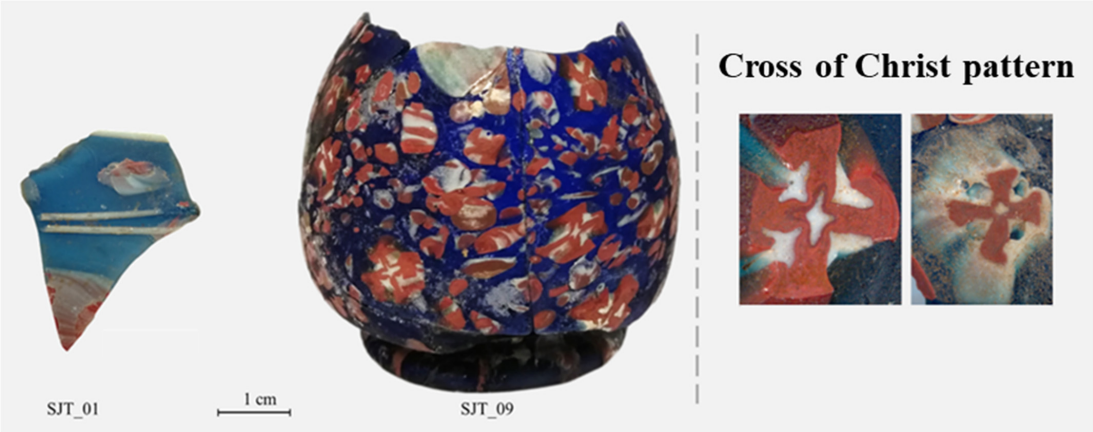

Figure 3. Selected *pick-up* glass fragments found in São João de Tarouca monastery to be analyzed.

Can some of these objects be considered local production? Indeed, these two archeological contexts have such high important glass assemblages, considering their diversity of forms, variety of glass objects, and decorative motifs; in recent decades, several works have been developed based on their glass artifacts [20,21,30–33].

2. Methodology

2.1. Sample Selection and Preparation

The selection of the glass fragments was carried out based on their representativity regarding morphological aspects such as: decorative patterns, range of colors, the shape of the original object, the presence/absence of layers of degradation, and the presence/absence of gold leaf.

To avoid erroneous results by analyzing and quantifying corrosion layers instead of the bulk glass, small samples (2–4 mm^2) were dry-cut with a diamond wire. These small samples were then embedded in an epoxy resin and polished with SiC sandpaper down to 4000 mesh. This sampling procedure was only performed on broken objects and on individual fragments without possible connections.

2.2. UV–Vis Absorbance and Reflectance Spectroscopy

UV–Visible absorption spectroscopy was used to confirm the presence of the transition metal ions responsible for the colors. An Avantes AvaSpec-2048 fiber optic spectrometer with a 300 lines/mm grating was used in the VICARTE research unit. The operational range was 350 to 1100 nm, and the instrument had a FWHM resolution of 2.4 nm. The light transmitted was measured using a 200 mm transmission probe (Avantes FC-UV600-2) with a diameter of 100 µm. The scattered light was collected with the fiber in direct contact with the glass sample.

2.3. µ-Raman Spectroscopy

Raman microscopy was carried out to aid in the identification of the opacifying crystalline compounds. A Labram 300 Jobin Yvon spectrometer equipped with an Nd:YAG laser 50 mW operating at 532 nm was used. Spectra were recorded as an extended scan. The laser beam was focused either with a 50× or a 100× Olympus objective lens. The laser power at the surface of the samples was varied with the aid of a set of neutral density filters (optical densities 0.3, 0.6, 1, and 2).

2.4. µ-PIXE

The micro-particle-induced X-ray emission (µ-PIXE) maps were useful to observe how the different elements were distributed throughout the different layers of glass. A PIXE with micrometer lateral resolution was performed using an Oxford Microbeams OM150-type scanning microprobe capable of both focusing down to 3 × 4 μm^2, the 1 MeV proton beam used, and scanning a sample surface area as large as 3730 × 3730 μm^2. The sample fragments were irradiated in a vacuum and a 30 mm^2 Bruker SDD X-ray detector with 145 eV energy resolution (at the energy of the Mn Kα line, 5.9 keV) was used for X-ray collection. Equipped with an 8 µm-thick Be window, it allows for detecting X-ray energies as low as the ones of Na while preventing most of the protons from entering and damaging the detector crystal. From the initially obtained 2D elemental distribution maps (with typical dimensions of 750 × 750 μm^2), the glass body and the several layers of different colors belonging to decoration were properly identified, and a representative region of interest was selected to visualize the distribution of different oxides throughout the layers. The equipment is located at the C2TN, Instituto Superior Técnico, Universidade de Lisboa, and was operated by Luís Cerqueira Alves.

2.5. LA-ICP-MS

Laser Ablation Inductive Coupled Plasma Mass Spectrometry (LA-ICP-MS) was used to obtain all the chemical compositions of the different glass layers. This technique has an

increased detection limit (can go to ng/g) that allows for measuring the major and minor elements and trace elements (including rare earth elements (REEs)), which makes it better suited for provenance studies [34]. This method is particularly well adapted to composite or decorated glass objects [35].

The glass objects are placed inside an ablation cell (Resonetics S155, 10 × 15 cm), where a micro-sample, invisible to the naked eye (diameter < 100 µm), is extracted by the laser beam. This sampled material is then carried to the plasma torch of the mass spectrometer by an argon/helium gas flow (1 L/min Ar + 0.65 L/min He) where it is dissociated and ionized by the high temperature of the plasma (8000 °C). The different glass constituents are separated according to their mass/charge ratios by the double-focusing mass spectrometer and quantified by the electronic detector (a secondary electrons multiplier or a Faraday cup according to the ion beam intensities).

The instrumentation employed consists of a Resonetics M50E excimer laser working at 193 nm, coupled with a Thermo Fisher Scientific ELEMENT XR mass spectrometer.

The excimer laser was operated at 5 mJ, with a repetition rate of 10 Hz. The beam diameter was adjusted from 40 µm to 100 µm to avoid saturation from elements such as manganese, cooper, tin, antimony, or lead. A pre-ablation time of 20 s was set in order to eliminate the transient part of the signal, which was then acquired for 27 s corresponding to 9 mass scans from lithium to uranium (the signal in count/second is measured in a low-resolution mode for 58 different isotopes). Between one and three ablations were carried out for each color of glass. If surface contamination was observed, a second or a third ablation was carried out at the same place.

Calibration was performed using 5 reference glass materials: (1) NIST610, (2) Corning B, (3) Corning C, (4) Corning D, and (5) APL1 (an in-house, standard glass with its composition determined by a Fast Neutron Activation Analysis, which is used for chlorine quantification), which were run periodically to correct for potential drift. The standards are used to calculate the response coefficient (k) of each element [35]. The net signals measured for each isotope are then normalized to ^{28}Si, the internal standard, and corrected for their isotopic abundance, their response coefficient, and their main oxidation state in order to calculate the concentration of each element expressed as oxide weight percentages (wt%).

The detection limits range from 0.1 to 0.01 wt% for major elements and from 20 to 500 µg/g for others.

To validate the obtained concentration results, glass reference standards Corning A and Nist 612 were regularly analyzed as unknown samples throughout all the analytical sequence. The average values obtained during the analysis for these glasses agree within 5 to 10% with the certified ones (for detailed information about the glass materials used for the calibration, please see Table S2 of the Supplementary Material).

3. Results and Discussion

3.1. Base Glass

This part of the work will begin by examining the base glass of the samples only. Each color or layer of different glass is considered separately. To achieve the base glass of our samples, the oxides associated with colorants (such as cobalt, copper, iron, and manganese), opacifiers (including antimony and tin), and other related elements (such as arsenic, bismuth, lead, nickel, etc.) were subtracted from the main composition and then normalized to 100%.

This base-glass methodology has been used in colored glass investigation as representative of the original clear glass, enabling a comparison of the main oxides with coeval Venetian and *façon-de-Venise* glass published in the literature, e.g., [20,36,37]. To uniformize all the glass layers, the iron oxide was removed from the "base glass", as it was usually added for coloring purposes. On the other hand, it is known that some oxides like Fe_2O_3 or MnO could also be unintentionally introduced in the glass matrix through raw materials; the presence of these oxides will be discussed later (Section 3.3.1).

The average, minimum, and maximum values of base composition are presented in Table 1 (for the complete composition, check Table S2 in the Supplementary Material).

Table 1. A presentation of the average, minimum, and maximum values of the base glass for clear and colored glass (presented in wt%) of the reduced glass composition (calculated by subtracting the colorants, opacifiers, and correlated elements and then normalizing it to 100%). All the presented values were acquired through LA-ICP-MS analyses.

Context	N° Samples	Color	Type of Inf.	Na_2O	MgO	Al_2O_3	SiO_2	P_2O_5	Cl	K_2O	CaO	TiO_2
SCV	19	Blue (t)	Average	16.0	2.9	3.2	63.3	0.35	0.96	4.21	7.50	0.14
		Blue (t)	Minimum	11.0	1.9	0.9	31.3	0.22	0.68	2.22	4.53	0.05
		Blue (t)	Maximum	18.8	3.6	7.0	70.0	0.48	1.28	7.46	10.18	0.29
SJT	2	Blue (t)	Average	13.4	3.65	3.95	59.9	0.375	0.67	7.41	10.63	0.11
		Blue (t)	Minimum	12.7	3.6	3.5	59.1	0.33	0.65	7.34	9.73	0.08
		Blue (t)	Maximum	14.0	3.7	4.4	60.6	0.42	0.69	7.48	11.52	0.14
SCV	9	Clear (tp)	Average	16.6	3.7	5.4	62.4	0.42	0.95	3.69	6.63	0.21
		Clear (tp)	Minimum	14.2	1.9	1.6	57.0	0.23	0.7	0.73	3.33	0.07
		Clear (tp)	Maximum	21.3	7.1	7.7	67.2	0.84	1.3	6.89	8.99	0.34
SCV	1	Green (t)	--	11.1	3.2	2.2	66.7	0.26	0.85	5.01	10.48	0.08
SCV	1	Purple (op)	--	15.9	2.7	3.4	65.8	0.48	0.88	3.92	6.74	0.15
SCV	15	Red (op)	Average	15.5	3.4	3.2	64.1	0.40	0.87	3.96	8.42	0.14
		Red (op)	Minimum	11.1	2.7	1.2	58.1	0.28	0.72	2.38	6.73	0.05
		Red (op)	Maximum	17.9	3.9	7.4	69.1	0.57	1.09	5.79	10.66	0.35
SJT	2	Red (op)	Average	14.5	3.5	3.9	60.5	0.39	0.67	7.14	9.43	0.10
		Red (op)	Minimum	14.6	3.7	4.1	60.6	0.41	0.72	7.52	9.61	0.12
		Red (op)	Maximum	14.3	3.3	3.6	60.3	0.36	0.62	6.76	9.25	0.08
SCV	9	Turquoise (t)	Average	15.3	3.1	3.2	65.7	0.36	0.95	4.20	7.38	0.12
		Turquoise (t)	Minimum	10.0	2.0	1.0	62.3	0.28	0.63	2.94	6.22	0.04
		Turquoise (t)	Maximum	18.5	4.6	5.2	70.1	0.43	1.18	6.73	9.29	0.18
SJT	1	Turquoise (t)	--	12.9	3.7	5.1	58.4	0.38	0.78	7.29	11.29	0.17
SCV	14	White (op)	Average	16.2	2.75	2.8	65.4	0.45	1.24	3.94	7.02	0.14
		White (op)	Minimum	11.2	1.6	0.9	61.4	0.29	0.71	2.27	4.21	0.04
		White (op)	Maximum	19.4	3.5	5.9	69.9	0.90	2.22	5.67	10.17	0.25
SJT	2	White (op)	Average	14.5	3.6	2.9	62.3	0.36	0.965	6.69	8.7	0.08
		White (op)	Minimum	13.9	3.5	2.7	61.9	0.34	0.87	6.03	8.47	0.07
		White (op)	Maximum	15.0	3.7	3.1	62.6	0.38	1.06	7.35	8.93	0.09

(t) = Translucent; (tp) = Transparent; (op) = Opaque.

Note that the content of PbO and SnO_2 in white layers has a representativity of about 29 wt% (between 16 and 44 wt%) because the amount of PbO and SnO_2. This value is considerably high when compared to the clear- and the other-colored glass layers, where the amount of reduced oxides are, on average, about 4 wt% (Table 2). This means that, for white-colored glass, the estimated "original clear glass" will be less reliable than for the other glass layers. The authors accepted this reality and decided to present and discuss the white glass layers along with the other clear and colored glass layers.

Table 2. Presentation of the average, minimum, and maximum values of the analyzed glass layers of SCV and SJT contexts determined by LA-ICP-MS. The oxides up to iron oxide are presented in weight percent (wt%), and the remaining oxides are presented in μg/g.

				wt%										μg/g										
Context	**N° Layers**	**Color**	**Type of Inf.**	**Na_2O**	**MgO**	**Al_2O_3**	**SiO_2**	**P_2O_5**	**Cl**	**K_2O**	**CaO**	**TiO_2**	**MnO**	**Fe_2O_3**	**CoO**	**NiO**	**CuO**	**ZnO**	**As_2O_3**	**SnO_2**	**Sb_2O_3**	**SrO**	**ZrO_2**	**BaO**	**PbO**	**Bi**
SCV	19	B (t)	Average	15.5	2.8	3.1	63.1	0.34	0.94	4.09	7.29	0.14	0.46	1.03	1692	510	1028	95	2354	2179	<10	514	65	248	1486	1069
		B (t)	Minimum	10.4	1.8	0.9	56.7	0.22	0.67	2.18	4.42	0.05	0.02	0.44	358	85	36	47	500	66	<10	206	23	75	2.32	124
		B (t)	Maximum	18.4	3.6	6.4	68.8	0.46	1.26	7.4	10.02	0.28	0.78	1.81	5118	1514	5906	197	6556	12,489	52	733	126	467	6531	5131
SJT	2	B (t)	Average	13.1	3.6	3.9	58.5	0.37	0.66	7.24	10.38	0.11	0.54	1.035	1240	385	150	150	2346	466	<10	854	58	12	451	307
		B (t)	Minimum	12.4	3.5	3.4	57.7	0.32	0.64	7.17	9.5	0.08	0.49	0.87	627	82	55	55	1806	187	<10	737	46	12	210	109
		B (t)	Maximum	13.7	3.6	4.3	59.2	0.41	0.67	7.3	11.26	0.14	0.59	1.2	1853	689	246	246	2887	745	<10	971	71	12	692	506
SCV	9	Cl (tp)	Average	16.2	3.6	4.7	60.6	0.40	0.92	3.60	6.81	0.21	0.54	1.05	57	34	2101	77	202	7227	<10	504	129	309	4813	57
		Cl (tp)	Minimum	14	1.8	1.4	55.2	0.23	0.69	1.34	3.24	0.07	0.22	0.55	10	11	12	39	20	130	<10	240	33	131	10	26
		Cl (tp)	Maximum	20.2	6.8	7.5	64.7	0.81	1.26	6.77	8.83	0.32	1.07	2.11	185	92	9500	132	544	29,433	<10	660	284	443	26,083	88
SCV	1	G (t)	--	17.5	3.1	2.2	65.1	0.25	0.83	4.88	10.21	0.07	0.4	0.94	163	69	2287	65	264	4236	19	551	54	231	3489	178
SCV	1	P (op)	--	16.2	2.6	3.3	63.6	0.47	0.85	3.79	6.52	0.15	0.76	1.34	2998	847	473	189	3220	735	<10	528	70	458	533	1489
SCV	15	R (op)	Average	14.0	3.1	3.1	58.7	0.37	0.81	3.53	7.10	0.13	0.37	3.19	193	101	11,514	221	420	13,906	34	494	107	184	17,031	170
		R (op)	Minimum	10.2	2.8	1.1	55.2	0.26	0.64	2.02	6.39	0.05	0.02	0.98	20	29	4640	32	52	484	26	286	23	76	516	11
		R (op)	Maximum	16.8	3.5	7.1	64.4	0.55	0.99	5.26	9.48	0.34	0.77	4.70	741	363	24,732	2158	1696	47,149	41	714	466	354	60,600	1039
SJT	2	R (op)	Average	13.7	3.4	3.7	57.5	0.37	0.64	6.80	9.10	0.10	0.45	3.15	63	29	9902	59	157	671	52	637	56	260	671	26
		R (op)	Minimum	13.5	3.2	3.4	57.3	0.34	0.59	6.44	8.80	0.08	0.44	2.71	59	28	6488	50	97	629	30	582	46	253	651	17
		R (op)	Maximum	13.9	3.5	3.9	57.7	0.39	0.69	7.15	9.13	0.11	0.46	3.58	68	31	13,316	69	217	714	114	692	66	267	691	36
SCV	9	T (t)	Average	14.2	2.6	2.9	61.0	0.34	0.94	3.91	6.75	0.12	0.33	0.80	704	226	30,335	83	902	3185	160	499	63	172	12,961	387
		T (t)	Minimum	9.0	1.6	0.7	55.4	0.23	0.57	2.43	5.52	0.03	0.02	0.01	30	33	1185	51	50	11	16	319	15	75	276	15
		T (t)	Maximum	17.7	3.3	4.7	67.3	0.42	1.6	6.09	8.7	0.17	0.77	1.55	5153	1483	79,704	126	6805	20,708	385	592	96	279	88,852	3197
SJT	1	T (t)	--	12.6	3.6	5	56.9	0.37	0.76	7.1	11	0.16	0.57	1.39	777	70	480	22	1942	212	236	915	87	251	446	79
SCV	14	W (op)	Average	11.4	2.0	1.9	46.4	0.32	0.86	2.8	5.05	0.09	0.26	0.58	53	52	3131	61	177	13	71	346	56	118	14	70
		W (op)	Minimum	8.0	1.1	0.6	37.2	0.21	0.55	1.91	2.36	0.03	0.07	0.33	12	22	115	21	37	<10	24	168	16	63	<10	10
		W (op)	Maximum	14.9	2.9	4.0	56.4	0.71	1.75	4.56	8.54	0.17	0.78	0.90	247	132	22,723	99	678	30	162	601	199	252	20	395
SJT	2	W (op)	Average	10.9	2.7	2.2	46.9	0.27	0.73	5.03	6.55	0.06	0.23	0.58	47	38	2259	41	205	9	81	468	34	143	13	30
		W (op)	Minimum	10.3	2.6	2.1	45.9	0.26	0.65	4.61	6.47	0.05	0.22	0.57	42	30	113	36	190	7	78	455	32	143	12	17
		W (op)	Maximum	11.5	2.8	2.3	47.9	0.28	0.81	5.45	6.62	0.06	0.23	0.58	52	47	4406	47	221	12	85	481	37	144	14	43

B = Blue; Cl= Clear; G = Green; P = Purple; R= Red; T= Turquoise; W= White; (t) = Translucent; (tp) =Transparent; (op) = Opaque.

3.1.1. Alkali Sources

All the analyzed glass samples have contents of Na_2O between 10.0 and 21.2 wt%, K_2O of 0.7–7.5 wt%, and CaO of 3.33–11.52 wt%. These results are compatible with soda–lime–silica glass types, which were profusely used by Venetian glass makers and in most of the Mediterranean *façon-de-Venise* production centers of the 16th and 17th centuries. This type of glass was made by using halophytic plants (that grow in salty soils) ashes as fluxing agent.

To distinguish and predict different kinds of glass based on the type of ash used as raw material in glassmaking, a normalization of fluxing oxides has been profusely used, e.g., [21,38,39]. Na_2O^* and K_2O^* are calculated by dividing the respective oxides by the oxides associated with the fluxing agent (Na_2O, MgO, P_2O_5, K_2O, and CaO), and the two correlated lines of $Na_2O^* + K_2O^* = 0.6$ and $Na_2O^* + K_2O^* = 0.75$ represent, respectively, the use of unpurified and purified ashes [10]. With this normalization, the influence of the ratio of fluxing agent and silica sources is eliminated [40].

As expected, due to the results of previous studies where SCV glass fragments were chemically investigated [17,20,21], these glass fragments also appeared dispersed throughout the different groups of sodic alkali sources (Figure 4). In the SCV context, glass composition comparable to the Venetian and *façon-de-Venise* production were already detected in *splashed* and *millefiori* [20], *filigrana* [21], gourd-shaped vessels [17], amongst others.

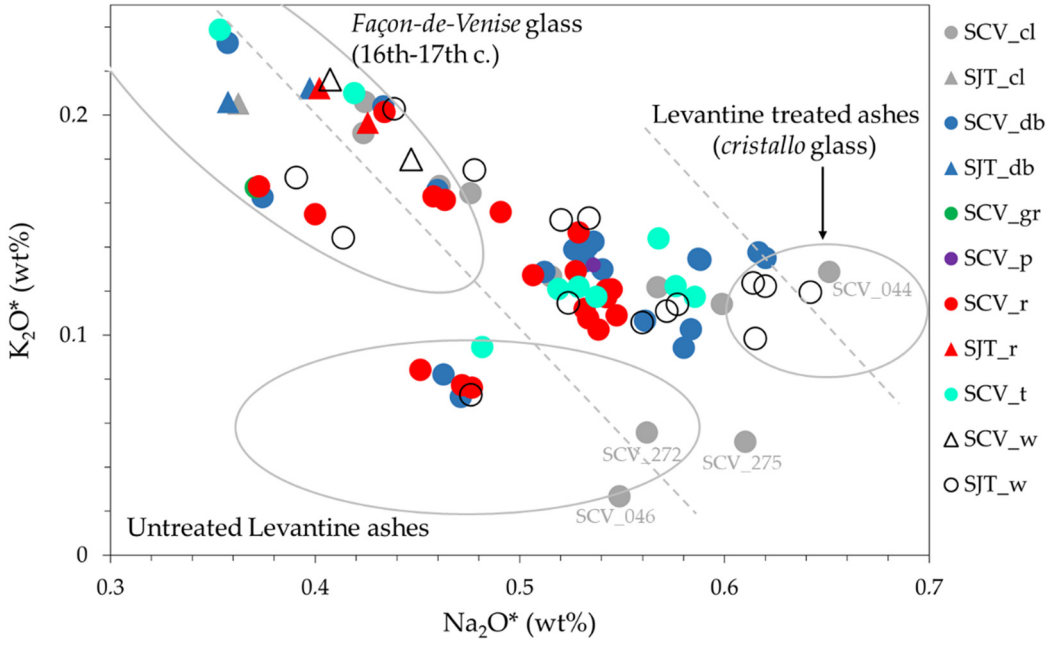

Figure 4. Base glass composition normalized to Na_2O^* ($Na_2O/(MgO + P_2O_5 + K_2O + CaO)$) and K_2O^* ($K_2O/(Na_2O + MgO + P_2O_5 + CaO)$) plotted with the correlation lines $Na_2O^* + K_2O^* = 0.6$ (untreated ashes) and 0.75 (treated ashes), indicating the use of, respectively, unpurified and purified ashes. cl = clear; db = dark blue; gr = green; p = purple; r = red; t = turquoise; w = white.

Considering the alkali sources (Figure 4), clear glass from SCV_044, 046, 272, 275, and 394 (*murrine*); dark blue glass layer from SCV_250, 365 (body), 366, and 368 (body); red glass from SCV 235 and 275; turquoise glass from SCV 250; and white glass from SCV_250, 365, 368, 388, and 394 were produced by using Levantine plant ashes, which makes these candidates to a genuine Venetian origin. The underlined numbers represent the analyzed glass samples which exhibit a composition that is compatible with *cristallo* glass (purified Levantine ashes). Moreover, clear glass from SCV_235, 236, 245, and 364 (*millefiori* cane); blue glasses from SCV_232 (body), 329 (body), and 364; green glass from SCV_232; red glasses from SCV_232, 245, 329, and 364; turquoise glasses from SCV_329 and 364; and white glasses from SCV_232, 245, 250, 329, and 364 are in the 16th and 17th

century *façon-de-Venise* glass region (Figure 4), meaning that they were probably using other fluxing agents like *barilla*.

The possible interpretation for the presence of samples between the two correlated lines (Figure 4) are the use of (1) a semi-purified ashes, (2) different recipes, (3) cullet, and (4) a mixture of sodic plant ashes.

Indeed, different plants have different contents of specific elements. For instance, *Barilla*, a native plant to the western Mediterranean, known as *Maçacote* in Portuguese or *Salsola Kali* in Latin, has a higher content of K_2O and was extensively used as a flux agent in the Iberian Peninsula, Sicily, and Sardinia, while Venetian glassmakers usually made a careful selection of the raw materials, importing them from specific locations such as Syria and Egypt (Levantine plant ashes) for the purer alkali sources (less K_2O) and the quartz pebbles from the Ticino or Adige rivers [9,41–43].

Although the enrichment of potassium oxide content is being linked to the flux agents (alkali sources) here, it is important to bear in mind that this higher amount of K_2O can also be related to other factors, like the use of silica sources rich in potassic feldspars or intentional addition of calcinated tartar (also known as *gripola di vino* or K-carbonates), which was widely used in the glass production since the 15th century [44].

In addition to this information, it is important to mention that, from the 15th century onwards, Venetian glassmakers also started to produce a new kind of glass (*cristallo* glass) by purifying the Levantine ashes to decrease the amount of impurities such as iron oxide, which were responsible for tinting the glass [45]. The disadvantage of this method is that, in the purification process, some glass stabilizers (e.g., CaO and MgO) were also removed, making the glass more susceptible to weathering degradation [46].

The detection of this purified composition has been noted in other production centers spread throughout Europe, e.g., [14,15,47,48], and has been considered a consequence of the immigration of some Muranese glassmakers during the 16th century. As a result of this emigration, the glass treatises and their subsequent translations made glass compositions and knowledge of the raw materials employed in glass making accessible to glassmakers all over Europe [42].

This information demonstrates that, although some glass layers appear in the *Levantine* ashes region (Figure 4), it does not mean that they were all made in Venice, as *Levantine* ashes were also used in other glass production centers outside of Venice.

Moreover, bearing in mind that the stability in the composition of the raw materials used in the best kind of Venetian glass has been considered essential to produce this high-quality glass [42], a Venetian attribution to the SJT and a greater part of the SCV fragments based on the alkali source is hard to propose, since the composition of 60 out of 75 (80%) of the analyzed layers are not compatible with Levantine ashes.

3.1.2. Silica Sources

Historical documents attest that Venetian glassmakers were using quartz pebbles from the Ticino and Adige rivers as silica sources [42,43]. On the other hand, in *façon-de-Venise* glass centers, glassmakers were usually using local silica sources for the glassmaking, e.g., [47–49]. Having this information in mind, the content of SiO_2, TiO_2, and Al_2O_3 can be of paramount importance in tracking the origin of raw material because they are the main components of silica sources.

For this part, the reduced composition (base glass, Table 2) is still used to compare our data with the data reported in the literature as the base glass has been considered closer to the original glass before the addition of glass colorants, e.g., [20,36,37].

In Figure 5, the chemical composition of the glass and the mineralogy of the glass-making sands are related. SiO_2 represents the quartz content, Al_2O_3 represents the amount of feldspars, and TiO_2 represents the heavy minerals present in silica sources [10,50]. In this graph, the area that was proposed to be the probable Lisbon production in Pulido Valente and co-authors' [18] work is marked. The possible Lisbon area has a higher amount of

feldspars when compared with the analyzed glass fragments from The Low Countries [51], Spain [10], and Venice [45,52].

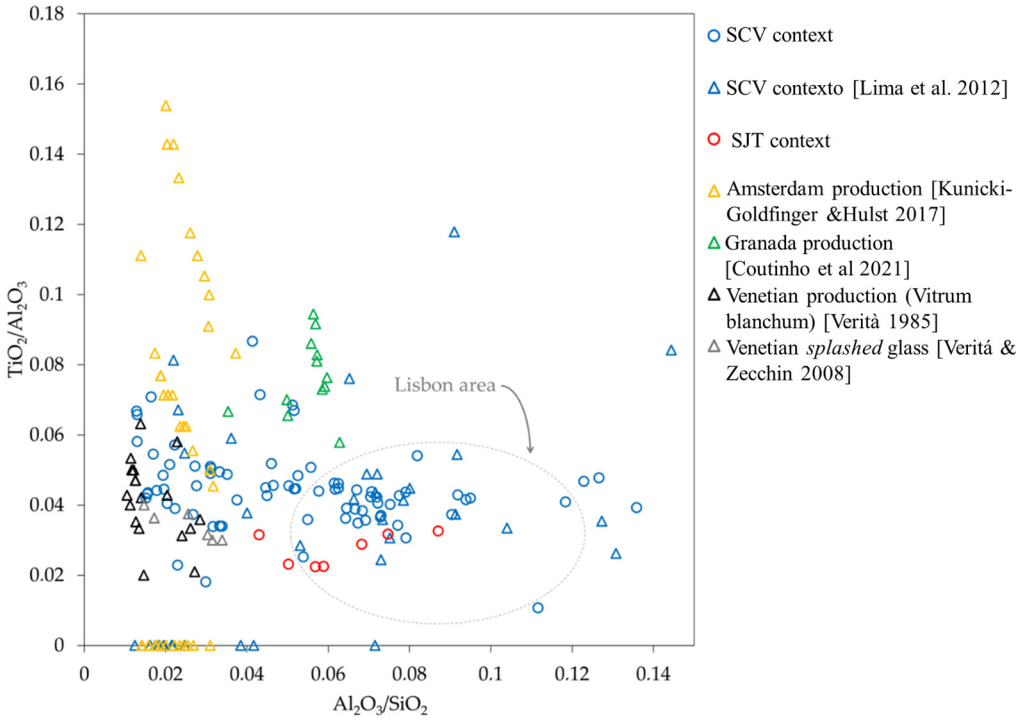

Figure 5. Binary plot of TiO_2/Al_2O_3 and Al_2O_3/SiO_2 of SCV (blue circle) and SJT (green circle) glass fragments treated in this article and some contemporary glass fragments reported in the literature. The clusters are grouped based on the mineralogy of the glass-making sands. The area of the graph that belongs to a probable Lisbon production was published by Pulido Valente and co-authors [10,18,20,45,51,52].

Interesting to highlight is the fact that the SJT assemblage is within or closer to the Lisbon area, and the SCV assemblages are spread through the graph. In the *millefiori* glass from the SCV context, including the previous work made by Augusta Lima and co-authors [20], about 50% of the glass layers (55 glass samples out of 113) are within the area previously proposed for Lisbon production.

In addition, while 3 glass layers analyzed by Lima and co-authors [20] do not match with any known glass production center, two layers belonging to blue glass body of SCV_365 and SCV_368 samples fall in the Granada region of the graph, and the remaining are distributed between Venetian and Dutch production.

From here onwards, the entire composition is being considered (e.g., with colorants, opacifiers, and related elements) (Table 2).

Figure 6 presents the relationship of zirconium (Zr) and hafnium (Hf). These elements have been extensively utilized to distinguish different sand quarries, as they are usually associated with felsic igneous rocks and are frequently used to distinguish different crustal processes because they are quite stable and resilient to chemical and mechanical destruction, e.g., [21,41,53]. It is broadly accepted that Venetian glass exhibits the lowest Zr content (<30 μg/g, whereas glass production centers of *façon-de-Venise* display higher levels of these elements [53–55]. This observation is linked to the fact that Venetian glassmakers enhanced the clarity of their glass by using high-quality raw materials, which include purer quartz sands, poorer in these elements [56].

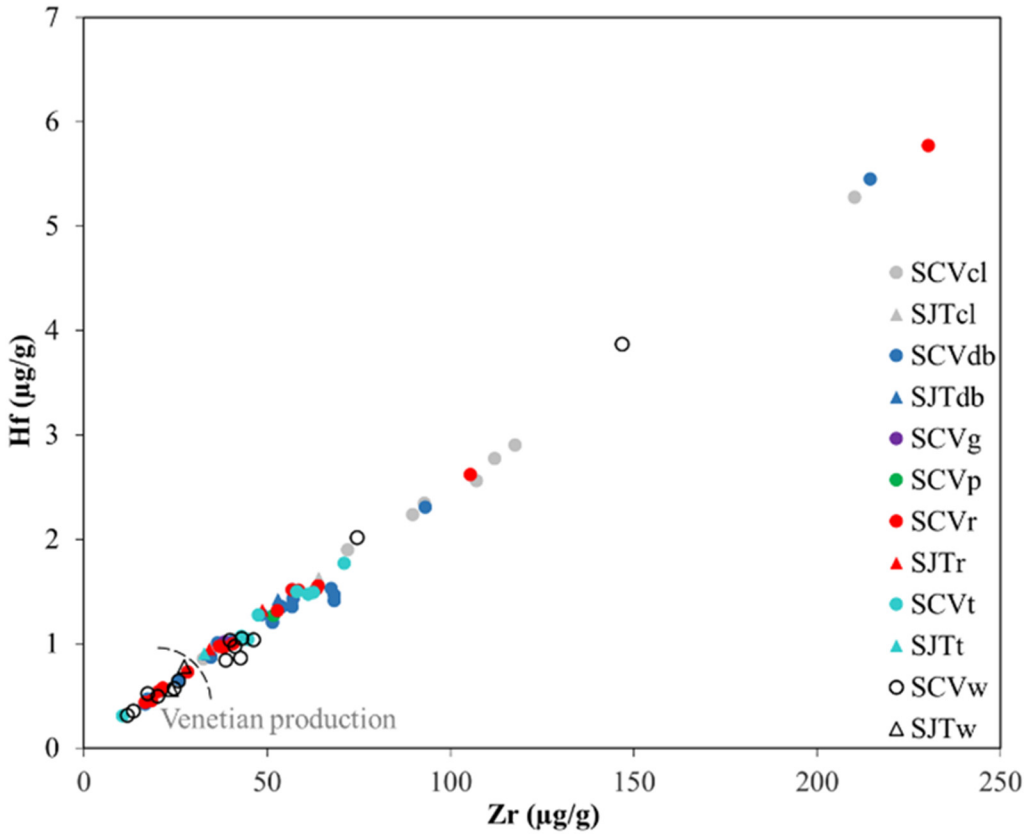

Figure 6. Binary chart of zirconium vs. hafnium, with the area of Venetian production marked in the chart [21,41,47]. cl = clear; db = dark blue; g = green; p = purple; r = red; t = turquoise; w = white.

To consolidate all the available data presented so far, it becomes evident that the number of glass layers associated with genuine Venetian production region on the graph can only be proposed for the following glass layers:

- Clear: SCV (394).
- Blue: SCV (250, 364, 366, and 394).
- Red: SCV (235, 250, 275 and 329).
- Turquoise: (SCV_364 and SCV_366).
- White: SCV (232, 250, 329, 360, 364, and 394); SJT (01 and 09).

3.2. Geochemical Patterns

Geochemical studies have been profusely used in provenance investigations because they are able to link the relative abundance of trace elements and REEs attributed to a certain region with the mineral origins of the silica sources used in glass production, e.g., [10,38,55,57].

Trace and REE analyses have also been employed in colored glass, as its REE contents in coloring do not significantly influence the geochemical patterns due to its insignificant amounts [58,59].

To obtain the geochemical pattern of a certain material, different normalizations can be made. In this case, the normalization of the considered trace elements and REEs was performed to (1) the upper Earth [60] and (2) carbonaceous chondrite normalization [60].

3.2.1. Normalization to Upper Earth

This normalization has been applied in some coeval glass provenance studies, e.g., [10,38,55,61].

Looking at the analyzed SCV and SJT samples normalized to the upper Earth crust, it was possible to identify four different geochemical patterns (GP) that can be seen in

Figure 7. This division was made by observing the deviations presented in the tendency line of each glass layer. The sample correspondence for each pattern is displayed in Table 3.

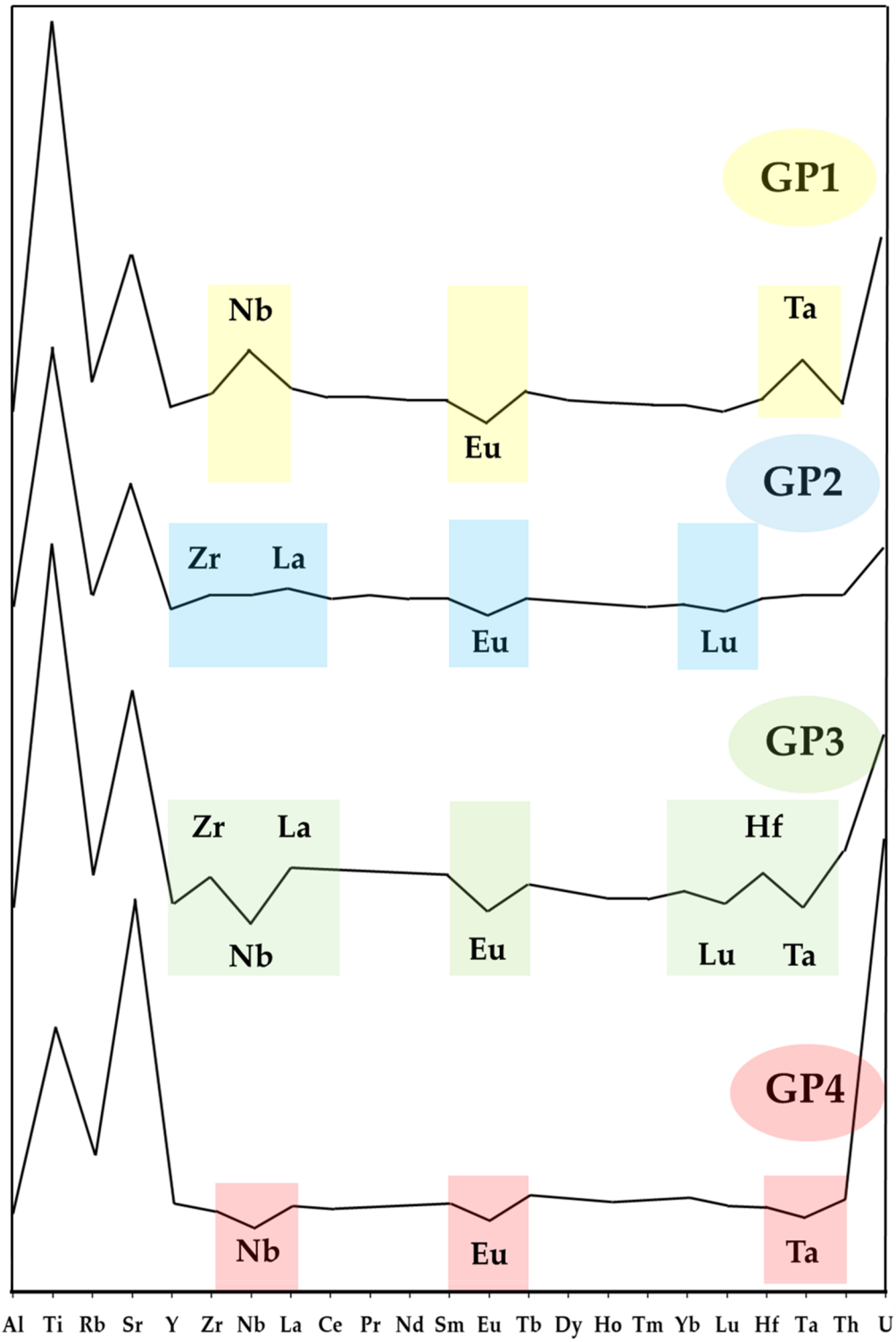

Figure 7. Representative geochemical patterns presented in logarithmic scale of trace elements and rare earth elements (REEs) found in SCV and SJT glass samples, normalized to Earth's upper crust.

The GP1 presents a positive anomaly in Nb and Eu elements and a negative anomaly in the Eu element.

Table 3. Attribution of each analyzed sample to its geochemical pattern (GP).

GP	Nº	Analyzed Glass Layer
1	4	SCV_365 (Body db/w), SCV_368 (Body db/w)
2	12	SCV_216 (r/t/w), SCV_365 (db/t), SCV_368 (db/p/t), SCV_388 (Body db/r/t/w)
3	30	SCV_044 (cl/db/r/w), SCV_235 (cl), SCV_236 (cl), SCV_245 (cl/db/r/w), SCV_250 (cl/tb), SCV_275 (cl), SCV_329 (Body db/tb), SCV_357 (db/r), SCV_360 (Body db/db/r/w), SCV_369 (Body db/db/r/t/w), SCV_375 (Body db/r/w), SCV_394 (Body db)
4	27	SCV_046 (cl), SCV_232 (db/gr/r/w), SCV_235 (r), SCV_250 (db/r/w), SCV_272 (cl), SCV_275 (r), SCV_329 (r/w), SCV_364 (cl/db/r/t/w), SCV_366 (db/t), SCV_394 (cl), SJT_01 (Body db/r/t/w), SJT_09 (db/r/w)

GP—geochemical patterns; Nº—number of different glass layers.

Interesting to note is that GP1 is represented by the glass body and white (decoration) layers of the SCV_365 and SCV_368 samples. These glass layers have similar ratios of Ti_2O/Al_2O_3 and Al_2O_3/SiO_2 when compared to the samples from Granada (Figure 5) [10]. Can this GP be attributed to Spanish/Iberian production?

GP2 displays a positive anomaly in Zr and La elements, while in Eu and Lu elements, a negative anomaly was noted. In this group are represented the remaining analyzed glass layers of the SCV_365 (db/t) and SCV_368 (db/p/t) samples and all the analyzed layers of the SCV_388 (db/r/t/w) and SCV_216 (r/t/w) samples. This geochemical pattern represents about 16% of all the glass layers analyzed.

The GP3 is the most popular PG, representing around 41% (30 out of 73) of the analyzed layers (Table 3). This specific geochemical pattern was previously identified in glass production waste recovered from Santana Convent and Largo do Chafariz de Dentro contexts (in Lisbon) and have also been detected in other contemporary Portuguese contexts located in Lisbon, such as the Rua do Arsenal site [21], Largo do Chafariz de Dentro site in *filigree* glassware [22], and in some glass vessels with a gourd shape found in SCV [17]. This characteristic indicates that all these glass fragments were probably made in the same glass production center, or, at least, a related silica source was used.

GP4 is characterized by having negative anomalies in Nb, Eu, and Ta elements; being the second most abundant GP of the analyzed glass layers, it is present in almost 37% of glass layers. All the analyzed samples belong to the SJT context (SJT_001 and SJT_009) plus 20 different glass layers of SCV monastery (Table 3).

It is worth mentioning that more than 57% of the analyzed fragments (42 out of 73) share the same geochemical pattern in all layers, including the glass body: SCV_216 and SCV_388 of GP2; SCV_044, SCV_345, SCV_360, SCV_369, and SCV_375 of GP3; SCV_232, SCV_364, SJT_001, and SJT_009 of GP4 (Table 3).

This evidence can indicate that, for the considered fragments, the *murrine* canes and the glass body of the object were probably made in the same glass production center. This is an interesting result because glass beads/canes and objects have been studied separately and usually by different researchers.

In three *pick-up* fragments (SCV_046, SCV_236, and SCV_272), only the glass body of the fragment was analyzed because the decoration layer could not be accessed. Moreover, the SJT_009 (t) and SCV_394 (r and w) layers were removed from this part because they do not fit in any previously grouped GP, so it was considered that they do not characterize this assemblage because they are probably outliers.

Noting that although four different geochemical patterns were observed, all the analyzed samples were characterized by the presence of a clear negative Eu anomaly (Figure 7). This evidence is being attributed to the separation of Eu^{2+} from Eu^{3+} in melts under low oxygen pressure, forming plagioclase minerals and substituting calcium [60].

3.2.2. Carbonaceous Chondrite Normalization

This normalization is useful for comparison, as it can provide complementary information about the redox conditions of the mineral formation and variations in sand composition used in the production of these artifacts [58].

A chondritic normalization approach provides insights into the elemental composition of these samples, revealing an enrichment in light rare earth elements (LREEs) compared to heavy rare earth elements (HREEs) and exhibiting negative Eu anomalies (Figure 8). While the range of the negative Eu element anomaly (Eu/Eu* between 0.14 and 0.93) may be considered substantial in the analyzed samples, it is significantly notable because it agrees with the dispersed values observed so far.

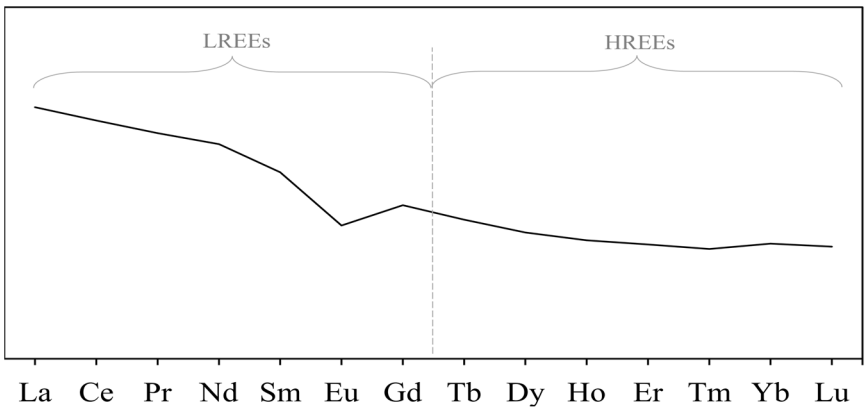

Figure 8. Pattern representation of the chondrite normalization to REE of SCV and SJT glass fragments.

The presence of this Eu anomaly, coupled with the concurrent enrichment of LREEs relative to HREEs, suggests that the silica sources used in the glass production originated from the weathering of granite-type rocks within the upper continental crust [57]. Moreover, weathered granite-type rocks with Eu/Eu* values ranging between 0.61 and 0.76 have been attributed to Venetian glass production [57,60].

Following this theory, about 40% of the samples from SCV and SJT archeological contexts (28 out of 76) present values of Eu/Eu* compatible with Venetian production (Table 4): SCV_044 (cl), SCV_216 (t), SCV_235 (cl), SCV_236 (cl), SCV_245 (cl/db), SCV_250 (db/r), SCV_272 (cl), SCV_275 (cl/r), SCV_357 (db/r), SCV_364 (db/r), SCV_365 (db), SCV_366 (t), SCV_368 (db/t), SCV_369 (db Body/db), SCV_375 (db/r), SCV_388 (db/r/t), SCV_394 (r), and SJT_001w.

Table 4. Information summarization related to the provenance investigation of SCV and SJT contexts.

Patterns	Samples	Alkali Sources (Na_2O^* vs. K_2O^*)	Silica Sources ($SiO_2/TiO_2/Al_2O_3$)	G P	Eu/Eu*
Splashed + rosette	**SCV_0044 cl**	Levant. (purified)	Near Lisbon region	3	0.48
	SCV_0044 b	Mix.	Lisbon	3	0.45
	SCV_0044 r	Mix	Near Lisbon region	3	0.49
	SCV_0044 w	Mix.	Lisbon	3	0.43
Splashed	**SCV_0046 cl**	Levant. (umpurified)	Near Lisbon region	4	**0.63**
Rosette	**SVC_216 t**	Mix.	Lisbon	2	**0.62**
	SCV_216 R	F.d.V.	Lisbon	2	0.33
	SCV_216 w	Mix.	Two Roses	2	n/d.
Indefinite	**SVC_232 b**	F.d.V.	Between Venetian and Two Roses	4	0.57

Table 4. *Cont.*

Patterns	Samples	Alkali Sources (Na_2O* vs. K_2O*)	Silica Sources ($SiO_2/TiO_2/Al_2O_3$)	G P	Eu/Eu*
	SCV_232 gr	F.d.V.	Venetian (Veritá and Zecchin 2008)	4	0.56
	SCV_232 r	F.d.V.	Venetian	4	0.56
	SCV_232 w	F.d.V.	Venetian	4	n/d.
Splashed	**SVC_235 cl**	F.d.V.	Lisbon	3	**0.62**
	SCV_235 r	Levant. (umpurified)	Between Venetian and Two Roses	4	0.28
Splashed + rosette	**SVC_236 cl**	F.d.V.	Lisbon	3	**0.72**
Indefinite	**SVC_245 cl**	F.d.V.	Lisbon	3	**0.69**
	SCV_245 b	Mix.	Lisbon	3	**0.61**
	SCV_245 r	F.d.V.	Lisbon	3	0.51
	SCV_245 w	F.d.V.	Lisbon	3	0.29
Splashed + rosette	**SVC_250 cl**	Mix.	Lisbon	3	0.52
	SCV_250 b	Levant. (umpurified)	Venetian	4	**0.70**
	SCV_250 r	F.d.V.	Venetian	4	**0.62**
	SCV_250 t	Levant. (umpurified)	Between Venetian and Two Roses	3	0.60
	SCV_250 w	F.d.V.	Between Venetian and Two Roses	4	0.14
Splashed	**SVC_272 cl**	Levant. (umpurified)	Near Lisbon region	4	**0.70**
Splashed	**SVC_275 cl**	Levant. (purified)	Lisbon	3	**0.61**
	SCV_275 r	Levant. (umpurified)	Venetian (Veritá and Zecchin 2008)	4	**0.70**
Splashed + hybrid	**SVC_329 b**	F.d.V.	Lisbon	3	0.53
	SCV_329 r	F.d.V.	Venetian	4	0.47
	SCV_329 t	F.d.V.	Lisbon	3	0.43
	SCV_329 w	F.d.V.	Venetian (Veritá and Zecchin 2008)	4	n/d.
Rosette	**SVC_357 b**	Mix.	Lisbon	3	**0.62**
	SCV_357 r	Mix.	Lisbon	3	**0.62**
Flowers + hybrid	**SVC_360 b**	Mix.	Two Roses	3	0.55
	SCV_360 b	Mix.	Two Roses	3	0.57
	SCV_360 r	Mix	Lisbon	3	0.59
	SCV_360 w	Mix.	Venetian (Veritá and Zecchin 2008)	3	n/d.
Murrine cane	**SCV_364 cl**	F.d.V.	Venetian	4	0.58
	SCV_364 b	F.d.V.	Venetian	4	**0.68**
	SCV_364 r	F.d.V.	Venetian	4	**0.64**
	SCV_364 t	F.d.V.	Venetian	4	0.58
	SCV_364 w	F.d.V.	Venetian	4	0.93
Flowers	**SVC_365 b**	Levant. (purified)	Granada (Coutinho et al., 2021)	1	0.78
	SCV_365 b	Mix.	Lisbon	2	**0.72**
	SCV_365 t	Mix.	Between Venetian and Two Roses	2	0.65
	SCV_365 w	Levant. (purified)	Between Two Roses and Granada	1	n/d.
Murrine cane	SCV_0366 b	Levant. (umpurified)	Venetian	4	0.77
	SCV_0366 t	F.d.V.	Venetian	4	**0.67**

Table 4. *Cont.*

Patterns	Samples	Alkali Sources (Na_2O* vs. K_2O*)	Silica Sources ($SiO_2/TiO_2/Al_2O_3$)	G P	Eu/Eu*
Flowers	**SVC_368 b**	Levant. (purified)	Granada (Coutinho et al., 2021)	1	0.78
	SCV_368 b	Mix.	Lisbon	2	**0.65**
	SCV_368 p	Mix.	Lisbon	2	0.59
	SCV_368 t	Mix.	Between Venetian and Two Roses	2	**0.61**
	SCV_368 w	Levant. (purified)	Between Two Roses and Granada	1	n/d.
Splashed + rosette	**SVC_369 b**	Mix.	Lisbon	3	**0.67**
	SCV_369 b	Mix.	Lisbon	3	**0.66**
	SCV_369 r	Mix.	Lisbon	3	0.54
	SCV_369 t	Mix.	Lisbon	3	0.50
	SCV_369 w	Mix.	Lisbon	3	n/d.
Rosette	**SVC_375 b**	Mix.	Lisbon	3	**0.69**
	SCV_375 r	Mix.	Lisbon	3	**0.65**
	SCV_375 w	Mix.	Lisbon	3	0.33
Indefinite + *rosette*	**SVC_388 b**	Mix.	Lisbon	2	**0.70**
	SCV_388 r	Mix.	Lisbon	2	**0.66**
	SCV_388 t	Mix.	Lisbon	2	**0.66**
	SCV_388 w	Levant. (purified)	Lisbon	2	0.18
Indefinite	**SVC_394 b**	Mix.	Between Venetian and Two Roses	4	0.49
	SVC_394 cl	Levant. (purified)	Lisbon	3	0.49
	SVC_394 r	Mix.	Two Roses	-	**0.65**
	SVC_394 w	Levant. (purified)	Between Venetian and Two Roses	-	n/d.
Rosette	**SJT_001 b**	F.d.V.	Lisbon	4	0.52
	SJT_001 r	F.d.V.	Lisbon	4	0.44
	SJT_001 t	F.d.V.	Lisbon	4	0.56
	SJT_001 w	F.d.V.	Between Venetian and Lisbon	4	0.61
Splashed + Rosette + Cross of Christ	**SJT_009 b**	F.d.V.	Lisbon	4	0.50
	SJT_009 r	F.d.V.	Lisbon	4	0.48
	SJT_009 w	F.d.V.	Between Venetian and Lisbon	4	0.17

cl = clear; b = blue; g = green; p = purple; r = red; t = turquoise; w = white. **Bold samples** represent the glass body layer. **Bold values of Eu/Eu*** represent the values that are compatible with Venetian glass production.

In the work developed by I. Coutinho and co-authors [62], some glasses were synthesized from sands and pebbles gathered from sedimentary deposits close to Coimbra and Côvo (Portuguese sites with documented glass production). In that work, the classification of silica sources as having granitic origin was also pointed out. The GP of those glasses were used to compare with historical samples, and three historical SCV glass samples studied presented on the work show a GP comparable with them. However, no SCV nor SJT *pick-up* glass fragments studied in this project present that pattern.

Interesting to note is when gathering the information of Eu/Eu* and the major oxides associated with silica sources ($SiO_2/Al_2O_3/TiO_2$) that present results comparable to Venetian production (SCV_250b, SCV_250r, SCV_275r, SCV_364b, SCV_364r, SCV_366b, and SCV_366t), more than 70% (5 out of 7) show the GP4 (upper Earth normalization). This observation reinforces the theory that GP4 can be possibly linked to Venetian production.

3.3. All Layers Together

The glass fragments analyzed in this study are more complex than other types of glass objects because they are composed of several layers of different colored glasses (glass body and the *murrina* that has several layers). As mentioned in the previous section, different objects are presenting different geochemical patterns in different layers. This observation reinforces the theory that the same cane could be made with different glass compositions/recopies. For this reason, in this section, elemental μ-PIXE mappings were used to better understand how the different elements related to colors are distributed through the glass layers.

In Figure 9, we can distinguish the different concentrations of iron, copper, and lead across the glass layers. These metals are associated with different colors/properties in glass. The presence of the heavy metal lead not only influences the opaque appearance of glass, but it can change its structure and hence its properties. SCV_375 presents a high concentration of lead in the opacified layers only, while in sample SCV_250, lead is more homogeneously distributed in the opacified layer and with a different concentration (in the red and colorless section). This could raise the big question of how the glass makers of 17th century knew that these different glasses were compatible with each other (e.g., thermal compatibility/similar expansion coefficient) if they did not know the composition of the different glasses.

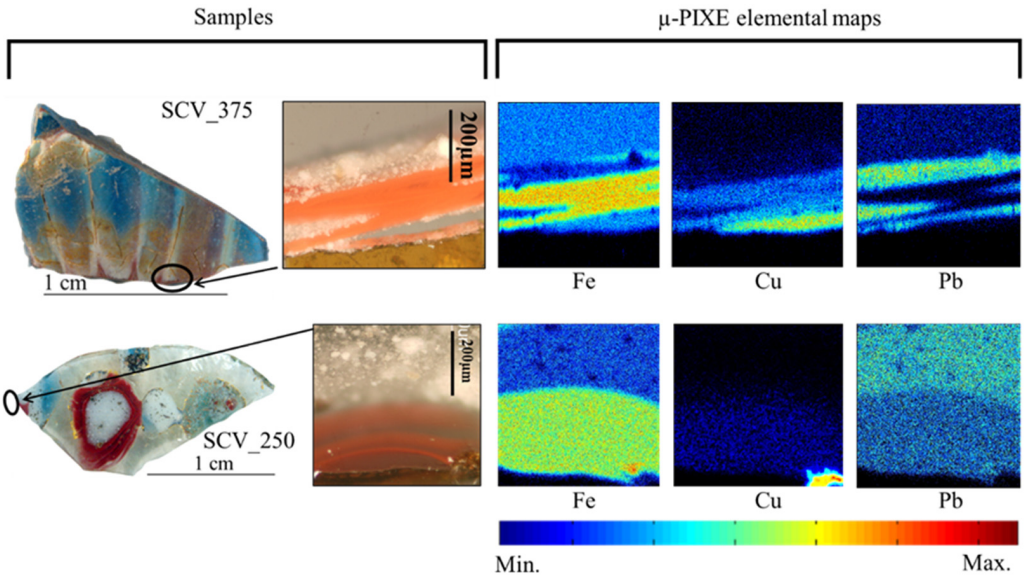

Figure 9. Elemental maps of SCV_375 and SCV_250 glass fragments acquired by using μ-PIXE.

Another notable characteristic shown by this technique is that in the red-colored layers of SCV_375, iron and copper present different concentrations: the lower layer has a higher content of Fe, while the upper layer has a higher content of Cu (Figure 9). For the red glass layer of the SCV_250 fragment, it is curious that while under the cross-section, different hues of red color can be distinguished, the μ-PIXE elementary maps do not provide any compositional distinction between them. This observation may be justified by the low size of cuprite crystals making the glass less homogeneous; this subject will be better discussed later when the red color is presented. The presentation and discussion of each color will be made in the following parts.

3.3.1. Naturally Colored Glass

In this section, clear glass encompasses all the glass that have "natural hues": almost clear and transparent (SCV_250); clear and translucent (SCV_235, SCV_236, and SCV_245); grayish tint (SCV_044); greenish (SCV_046 and SCV_394); and yellowish (SCV_272 and SCV_275).

Regarding the alkali sources, the clear glasses that fall within the "*Levantine plant ashes*" region (Figure 4) display distinct intense natural hues: (1) greenish in SCV_394 *murrine*, (2) grayish in the glass body of SCV_044 little flask fragment, (3) greenish in the glass body of SCV_046 gourd-shaped vessel fragment, and (4) yellowish in the glass body of SCV_272 and SCV_275 fragments. Additionally, the clear glass within the *façon-de-Venise* region appear more discolored (e.g., SCV_235, SCV_236, and SCV_245). More decolorized and transparent is the SCV_250 glass body, which falls between the two correlated lines. These observations open some questions, such as: (1) Can this observation indicate that "clear" glass that was produced with the Levantine ashes composition, based on its fluxing agent, is a result of glass recycling or the color is intentionally produced? (2) If the answer is yes, why? (3) Is it linked to aesthetic issues or the preservation purpose of its content?

Looking to MnO and Fe_2O_3 contents, we can start understanding how these oxides will influence each color (Figure 10).

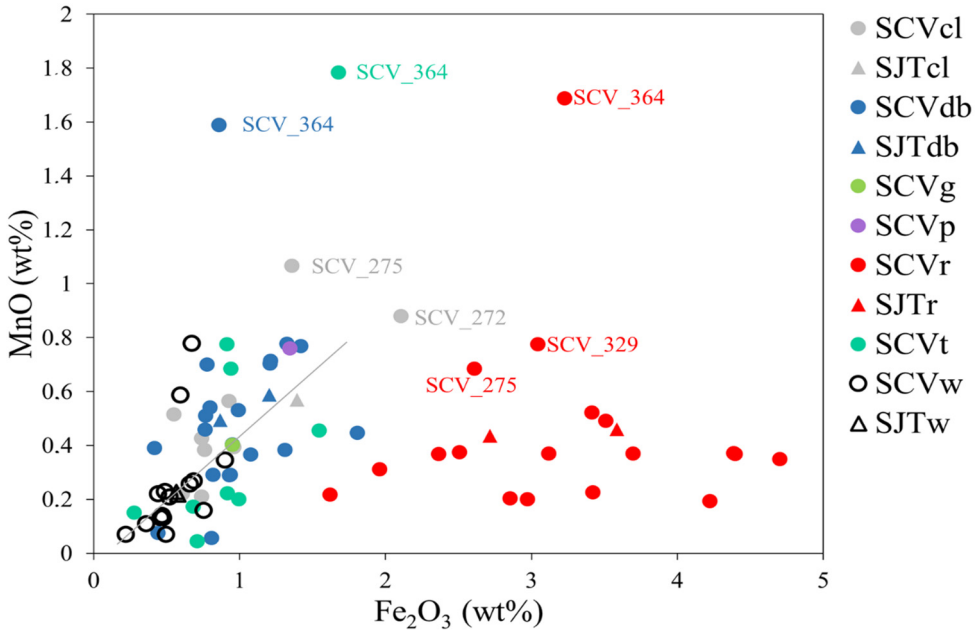

Figure 10. Binary chart of MnO vs. Fe_2O_3. * cl = clear; db = dark blue; g = green; p = purple; r = red; t = turquoise blue; w = white.

Iron and manganese oxides can be unintentionally introduced in the glass matrix through raw-materials or deliberately added by the glassmakers to make clear or colored glass. Figure 10 presents a positive correlation between Fe_2O_3 and MnO in most clear, blue, green, purple, and white glasses. This evidence suggests that their presence in the glass matrix is probably unintentional, having been introduced through the raw materials.

The yellowish glass body layers of SCV_272 and SCV_275 fragments exhibit the highest concentration of both oxides (approximately 1.5 wt% of Fe_2O_3 and around 1 wt% of MnO). As the amount of manganese oxide is closer to 1 wt% (value that has been attributed to intentional addition), it is probable that the final color can be considered as an intentional semi-discoloration of glass [38,44].

In glass, iron can give a color that ranges from bluish, when ferrous ions (Fe^{2+}) are predominant, to yellowish, when ferric ions (Fe^{3+}) are predominant. Usually, the iron oxide gives a wide range of green color due to the presence of both ions in the glass matrix [63,64].

To discolorize a glass, manganese oxide could be introduced in the glass batch (usually by adding pyrolusite [MnO_2]) which oxidates the iron oxide (from Fe^{2+} to Fe^{3+}) [63]:

$$2FeO + MnO_2 = MnO + Fe_2O_3$$

As a result, the final glass becomes grayish or achromatic because purple (produced by the residual amount of Mn^{3+}) and yellow (produced by the oxidation of Fe^{2+} to Fe^{3+}) are complementary colors.

Another possibility for this positive correlation (Figure 10) can be viewed as a recipe improvement whereas, the higher content of Fe_2O_3 in the glass batch requires an increased addition of MnO to oxidize the ferrous ion (Fe^{2+}) into ferric ion (Fe^{3+}) and thus convert MnO_2 into MnO (almost colorless) [20,63].

Manganese oxide also exhibits a strong coloring ability and can impart a deep purple hue, even at concentrations as low as 1.1 wt% when Mn^{3+} (Mn_2O_3) is prevalent [21]. However, its effects are highly dependent on the redox conditions within the furnace and the composition of the glass batch. Blue, red, and turquoise colors from the SCV_364 sample (*millefiori* cane) exhibit an MnO enrichment (around 1.7 wt%) when compared with other samples (Figure 10). This evidence can suggest that MnO was intentionally added into the glass batch to intensify the final color.

Finally, we observed that several natural hue samples present high concentrations of trace elements associated with (de)colorants (Mn, Co, Ni, Cu, Zn, As, Se, Ag, Cd, In, Sn, Sb, Au, Hg, and Pb oxides) between 100 and 1000 μg/g, which can be interpreted as glass recycling [56].

Based on this information, we can propose that the greenish color of SCV_0046 (small glass bottle with the Portuguese gourd shape) and SCV_394 (in the *murrine*) present recycling signs, as the content of PbO is higher than 1 wt%, and CuO and SnO_2 are near 1 wt%). Comparable amounts of PbO in clear glass fragments were previously reported in the literature on SCV glass fragments: (1) 2.83 wt% of PbO in the clear glass body of V_074 *splashed*-glass fragment (Figure 11) [20] and (2) 1.89 wt% of PbO in the glass body of the SCV_210 gourd-shaped vessel fragment [17].

Figure 11. Image of the glass fragment V_074 analyzed by Lima and co-authors [20].

For the same reason, in the SCV_0044 (small bottle displaying a gray glass body) sample, the content of CoO (148 μg/g), PbO (386 μg/g), and SnO_2 (363 μg/g) are compatible with glass recycling.

Surprisingly, the yellowish glass body of SCV_272 and SCV_275 fragments exhibit low concentrations of CuO, SnO_2, Sb_2O_3, and PbO (all below 10 μg/g), which can indicate that no cullet was used in the glass production of these glasses.

Among all the clearest samples (SCV_235, SCV_236, SCV_245, and SCV_250), two of them seem to be less pure, the SCV_236 and SCV_245. These samples present contents of PbO, SnO_2, and CuO (all above 100 μg/g), suggesting the addition of cullet to the raw materials, while the contents of these oxides on SCV_235 and SCV_250 samples are consistent with natural content coming through the raw materials.

In Figure 12, six UV–Vis absorption spectra of different clear glass bodies reveal the discernible influence of Co^{2+} and Fe^{2+} and Fe^{3+} ions within the glass matrix. The octahedral Fe^{2+} can be observed, with its broad band centered around 1100 nm, and tetrahedral Fe^{3+}

has typical absorption bands at 380 nm, 420 nm, and 440 nm [64]. Also, the presence of cobalt, mainly observed in SCV_236 and SCV_245 fragments (CoO = 73 ppm and 36 ppm, respectively), can be detected by the presence of the bands at 540 nm, 590 nm, and 640 nm.

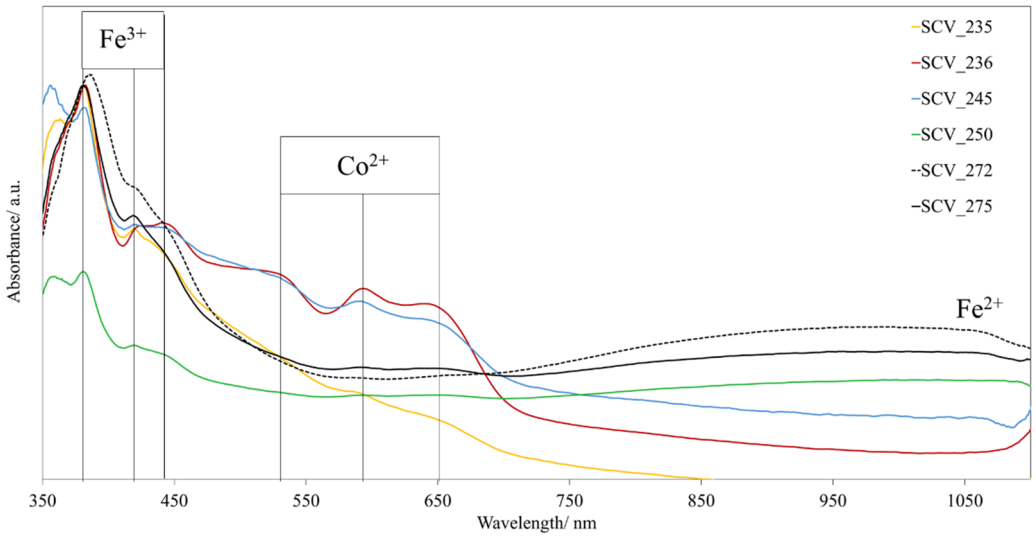

Figure 12. UV–Vis absorption spectrum of the clear glass body performed on SCV (235, 236, 245, 250, 272, and 275) fragments, revealing the discernible influence of Co^{2+} and Fe^{2+} and Fe^{3+} ions within the glass matrix.

It is interesting to point out that, according to M. Volf [63], small amounts of cobalt oxide could be intentionally added to the glass batch to remove the faint yellow color. Can this explain the high content of CoO, SnO_2, and PbO in the clear glass of the SCV_044 sample (by the addition of smalt)? Although the presence of cobalt oxide in clear glass is not common, it has been reported in few contemporaneous *façon de Venise* glasses found in Portugal, e.g., [21].

Both yellowish glass bodies (SCV_272 and SCV_275) are more influenced by iron ions than the colorless glass body of SCV_250, indicating that the clear glass bodies of SCV_236 and SCV_245 are clearly influenced by cobalt (73 μg/g and 36 μg/g, respectively) and iron (0.93 wt% and 0.76 wt%, respectively).

3.3.2. Colored Glass Layers

Concerning the colored glass, LA-ICP-MS, UV–Vis Absorbance and Reflectance Spectroscopies, and μ-RAMAN provided information about the colorants that were added to clear glass to color it: cobalt for blue, iron and copper for red, copper for turquoise, and a combination of lead and tin oxides (originating cassiterite clusters) for white. These colorants were very popular in contemporary glassmaking and several glass recipe books attest to their applications, e.g., Darduin, Dell'arte del vetro per musaico, Ricette vetrarie del Rinascimento (also known as Anonimo), Trattatelli [44,52,65].

BLUE

The blue color observed in *millefiori* glassware is attributed to the presence of CoO within the glass matrix. The analyzed assemblage reveals that all blue glass bodies from the SCV context and SJT_01 sample contain CoO values lower than 0.11 wt%. This content of cobalt oxide aligns with blue–blown glassware reported in the literature [52]. In contrast, the SJT_09 glass body (0.19 wt% of CoO) and all blue glasses used in the decoration display CoO levels ranging from 0.1 to 0.45 wt%. These values are comparable to those found in beads [57], enamels [36], and Portuguese, glazed tiles [66].

As pointed out in a Venetian *splashed* vessel studied by M. Verità and S. Zecchin [52], the CoO content detected in the decoration is typically higher than what is found in the

blue glass body because the original color of the decoration must be preserved even if it is applied thinly.

The UV–Vis absorbance spectroscopy analyses were performed in all blue layers of the selected samples to determine the ions that contribute to the final color of the blue and bluish glass layers.

Besides cobalt (Co^{2+}), the ions of copper (Cu^{2+}) and iron ($Fe^{2+/3+}$) also influence the blue glass layers of the examined artifacts, as illustrated in Figure 13 for the SCV_357, SCV_365, and SCV_400 samples.

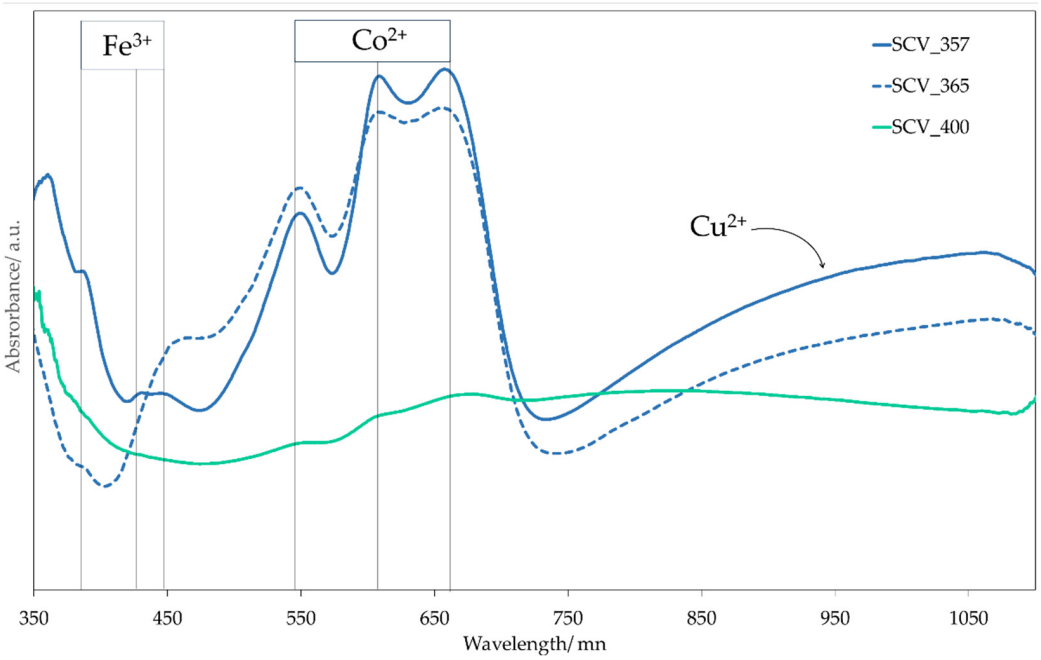

Figure 13. UV–Vis absorption spectrum of blue glass layers performed on SCV_357, SCV_265, and SCV_400 fragments revealing the discernible influence of cobalt (Co^{2+}), copper (Cu^{2+}), and iron (Fe^{3+}) ions within the glass matrix.

For all the presented blue glass bodies, a triple band located around 530 nm, 590 nm, and 640 nm can be observed. This triple band characterizes the cobalt ions in $3d^7$ electronic configuration with tetrahedral coordination [64]. Considering that the geometry of the ligand around the chromophore can slightly change in different glass samples, the shift of the three bands associated with Co^{2+} in soda–lime–silica glass appears at 535, 595, and 640 nm.

This configuration of cobalt ions has a high extinction coefficient and, for that reason, is very visible in the UV–Vis analysis even at very low concentrations, when compared with other techniques as, for instance, XRF, EDS, or PIXE [64,67].

Additionally, the spectra reveal other peaks related to iron. In SCV_357, the characteristic absorption bands of ferric ion (Fe^{3+}) at 380, 420, and 440 nm and the ferrous ion (Fe^{2+}) with its broad band at around 1100 nm [64] probably contributed to the hue. When viewed with the naked eye, SCV_357 and SCV_400 blue tones are quite similar.

To try to predict the origin of mineral cobalt, some oxides have been profusely used: NiO, ZnO, As_2O_3, and Bi, e.g., [37,68,69]. Apart from the SCV_394 fragment, all the blue samples have contents of NiO (0.009–0.12 wt%), ZnO (0.004–0.02 wt%), As_2O_3 (0.05–0.52 wt%), and Bi (0.01–0.51 wt%) associated with CoO. These results indicate that these objects were probably produced after the 1520/30 decade and that the cobalt ore was imported from Schneeberg, e.g., [37,68,69]. In contrast, the SCV_394 blue glass body has an absence of As_2O_3. This observation is viewed as a timeline indicator (before 1520/30) because it is linked with the calcination process of cobalt ore before its addition to the

glass batch, as the arsenic is a volatile oxide [68,69]. Due to this As_2O_3 absence, it is possible to propose that this glass object was probably produced before 1520/30 by using the oldest recipe.

GREEN

The green glass of the SCV_232 fragment is the consequence of the presence of Co^{2+} (CoO = 0.016 wt%) and Cu^{2+} (CuO = 0.229 wt%).

The content of PbO (0.35 wt%) and SnO_2 (0.42 wt%) suggests that cullet may have been used in this glass layer or that these elements were being diffused from the adjacent white layer during the working time, when the glassmaker fused the decoration to the glass body and manipulated the object being created.

In Figure 14, the first band of Co^{2+}, located at 540 nm, is nearly imperceptible at first glance. However, upon closer examination, a slight increase around 540 nm can be seen. The broad band of Cu^{2+} with a maximum wavelength located between 780 and 810 nm is also shown in Figure 14.

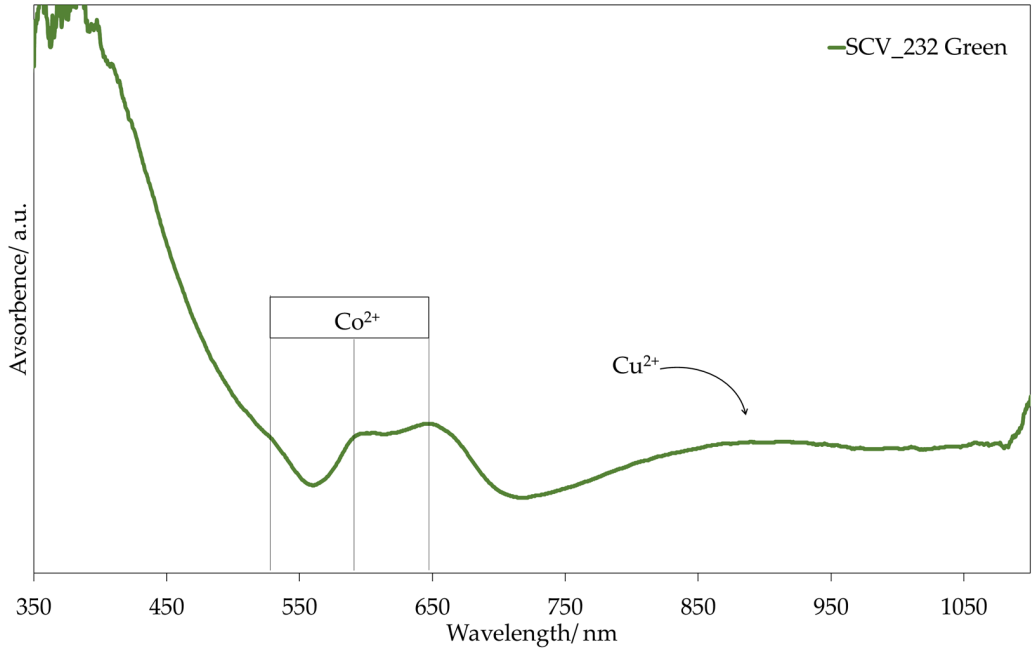

Figure 14. The UV–Vis absorption spectrum of green glass layer performed on the SCV_232 fragment revealing the discernible influence of cobalt (Co^{2+}) and copper (Cu^{2+}) ions within the glass matrix.

PURPLE

The analyzed purple glass layer of SCV_368 sample is almost black (Figure 15) and has the following amount of colored oxides: MnO = 0.76 wt%, Fe_2O_3 = 1.34 wt%, CoO = 0.30 wt%, CuO = 0.05 wt%, SnO_2 = 0.07 wt%, and PbO = 0.05 wt%. This spectrum is very saturated, so the bands representing the different ions are difficult to distinguish.

While the UV–Vis spectrum (Figure 15) is really saturated, presenting a broad band between 350 and 650 nm that masks the main chromophores, we can combine the chemical composition of the colorants with the information gathered from Figure 15. According to the consulted literature, Mn^{3+} presents a broad band at 450/500 nm that can mask the triple band of Co^{2+} located at 530, 590, and 640 nm by considering the sum of all the bands [64]; so, the spectrum is not incompatible with the presence of MnO, Fe_2O_3, CoO, and CuO, and it can be considered an envelope of the spectra of the respective ions, where the presence of Mn^{3+} and Co^{2+} is more apparent.

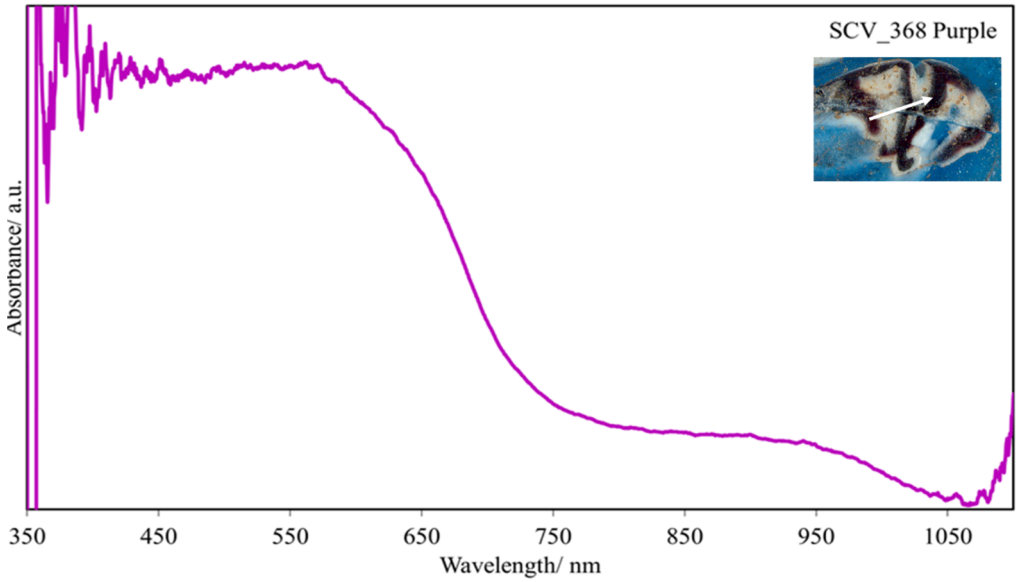

Figure 15. The UV–Vis absorption spectrum of the purple glass layer performed on the SCV_368 fragment revealing the discernible influence of cobalt (Co^{2+}) and manganese (MnO) ions within the glass matrix. The arrow is indicating the color of the sample.

RED

For all the analyzed red glass layers, the micro particles of copper were detected and, while this type of glass is tricky to produce, this color has been used since the Roman times [70,71].

In reduced conditions, metallic micro particles of copper (Cu^0) or crystals of cuprite (Cu_2O) precipitate on the glass matrix, and a red color is formed [20,70]. Historical recipes suggest that, besides copper oxide, glassmakers added, iron, antimony, lead, and tin oxides to the glass batch, as they can act as reducing agents [20,46,70].

The analyzed red samples show amounts of CuO (0. 59–2.41 wt%), Fe_2O_3 (0.98–4.70 wt%), SnO_2 (0.048–4.71 wt%), Sb_2O_3 (0.003–0.014 wt%), and PbO (0.05–6.06 wt%), which are compatible with those reported in the literature for coeval red glass artifacts, e.g., [20,52,71].

This type of glass is characterized by having a broad band around 330 and 770 nm in the UV–Vis absorption spectrum [64], as noted in all the red glasses analyzed in this project (Figure 16a).

In the SCV and SJT fragments, only the red decoration belonging to the SCV_245 sample presents several layers of red, turquoise, white, and clear glass under the cross-section (Figure 16b). Under the surface, it is possible to note that this decoration has several hues, probably indicating that these layers were intentionally produced. This observation may indicate that the SCV_245 fragment, initially attributed to a *splashed* glass, has a *millefiori* decoration; although, the drawing of the pattern is impossible to determine.

However, it is also plausible that this red glass layer was not so homogeneous, or the red–ox conditions were not enough to achieve the ideal conditions for the formation of nanoparticles of copper/cuprite [70]. Similar layers of red and transparent glass were also observed in a red glass body found in the Santana monastery in Lisbon [18].

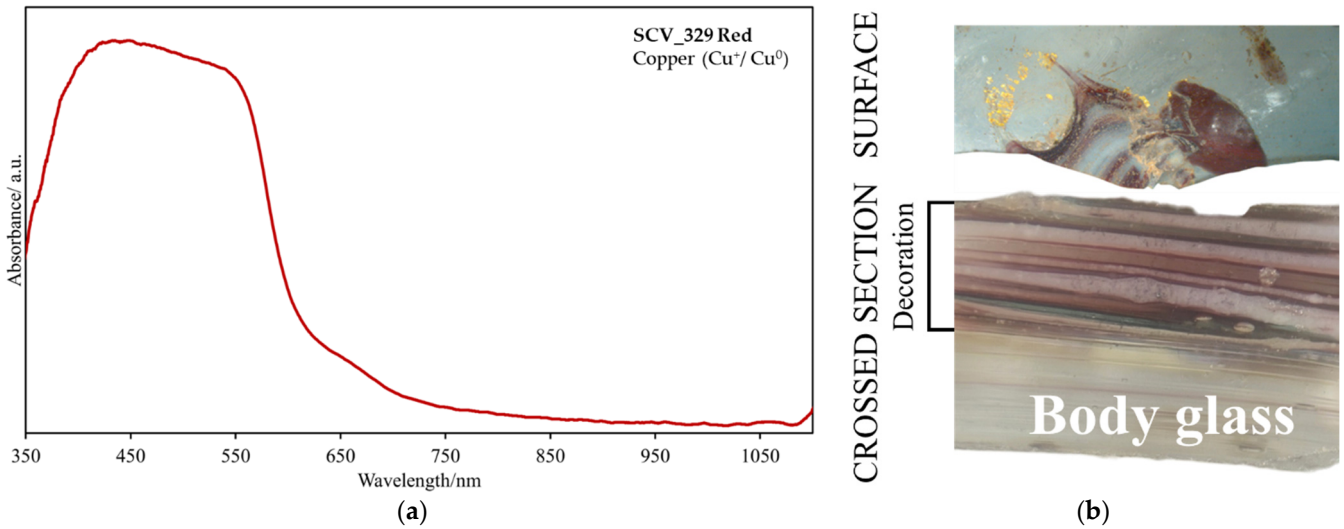

Figure 16. (**a**) UV–Vis absorption spectrum of red glass layer performed on SCV_329 fragment, revealing the discernible influence of monovalent (Cu^{+}) and metallic (Cu^{0}) copper. (**b**) Close-up of the SCV_245 fragment under the surface and cross-section.

TURQUOISE

The turquoise glass belonging to the selected SCV and SJT fragments have a CuO content between 0.19 and 7.97 wt%. This amount of copper oxide is in line with what has been reported in the literature for coeval *millefiori* glass [20] and glass beads [72] of the 15th and 17th centuries.

This color, produced by the presence of Cu^{2+} ion, is obtained under oxidizing conditions, and the characteristic broad band of UV–Vis absorption spectrum is located between 780 and 810 nm (Figure 17), which corresponds to octahedral coordination of a $3d^{9}$ electronical configuration [64,67,71].

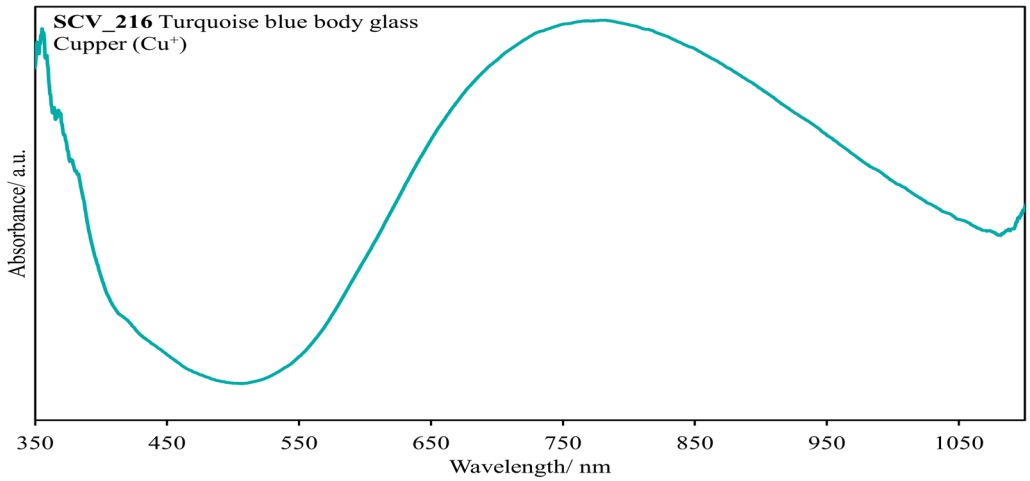

Figure 17. UV–Vis absorption spectrum of the turquoise glass body of the SCV_216 fragment revealing the discernible influence Cu^{2+} ions into the glass matrix.

As pointed by M. Costa and co-authors [57], the amount of PbO has a significant impact on the final turquoise color. Most of the analyzed fragments have low contents of lead oxide, ranging between 0.09 and 1.86 wt%, while the turquoise glass layer of SCV_366 (*millefiori* cane) have 8.16 wt% of PbO. Although this turquoise color may not appear visibly distinct from the others, simultaneous detection of SnO_2 (8.50 wt%) suggests that both lead and tin oxides were likely added to the glass batch for opacification purposes, as was also observed in some tubular blue glass beads of the Nueva Cadiz type unearthed in the

Lisbon city center [73]. The other fragments have SnO_2 contents that range between 0.06 and 2.07 wt%.

WHITE

In the 16th century, Venetian glassmakers were using tin- and antimony-based opacifiers to make white glass [20,52].

The white glass layers of the *pick-up* glass fragments of the SCV and SJT archeological contexts have SnO_2 (4.34–30.57 wt.%) and PbO (7.73–22.04 wt.%) and less than 0.01wt.% of Sb_2O_3 as major components, which indicates that all white samples were opacified with a tin-based component.

White opaque glass displays a notable heterogeneity, characterized by the presence of white opaque clusters of diverse sizes dispersed within the glass matrix (Figure 18a). The study of these opaque white particles was carried out via μ-Raman microscopy.

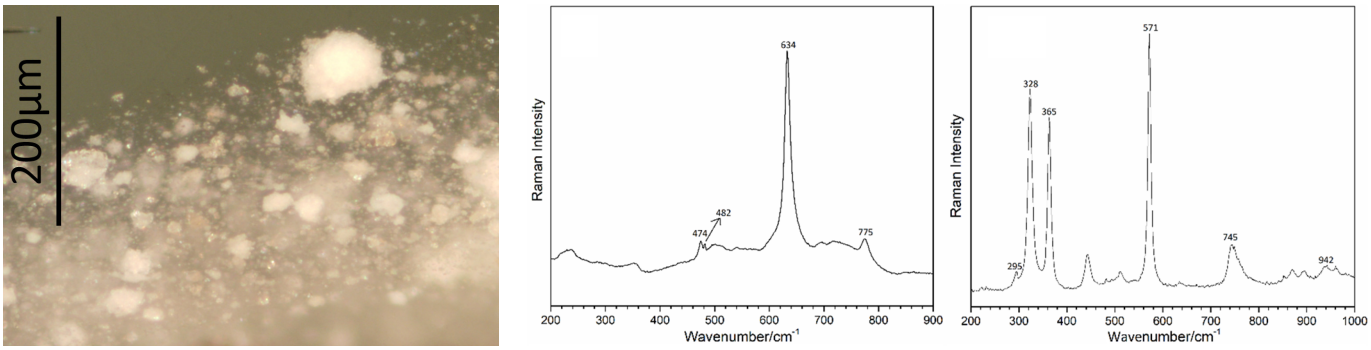

(**a**) (**b**) (**c**)

Figure 18. (**a**) Optical microscope image of the SCV_250 glass sample where the coarse, white particles can be observed. (**b**) Raman spectrum of cassiterite (SnO_2) and (**c**) Raman spectrum of malayaite ($CaSnOSiO_4$).

The Raman spectra performed on these white clusters allowed for the identification of the presence of cassiterite in all the analyzed samples and, for the SCV_245 and SCV_250 samples, some malayaite crystals were also detected (Figure 18b,c).

White, opaque glass opacified with cassiterite (tin dioxide) clusters was introduced in Venetian glass recipes at the beginning of the 15th century and began to be profusely used in the most important glass objects like in the white threads of *filigrana* glass canes, enamels, and to make *lattimo* glass, which imitated Chinese porcelain, e.g., [7,20,52,74].

This compound has a characteristic Raman signature at 635 cm^{-1} and 775 cm^{-1}, and, frequently, a less intense pike at 474 cm^{-1} can also be observed [20,21,75] (Figure 18b).

Cassiterite clusters were also detected in contemporaneous white glaze of Portuguese tiles [66], beads found in the African [57] and American [72] continents, enamels [36,37], and mosaic tesserae [65].

The presence of malayaite ($CaSnSiO_4$) in the SCV_245 and SCV_250 samples (Figure 18c) is confirmed by its characteristic Raman bands at 571 cm^{-1}, 365 cm^{-1}, and 322 cm^{-1} [76]. The formation of this tin mineral is a consequence of the presence of equimolar parts of CaO, SiO_2, and SnO_2 and its development can be favored in the presence of transition metal ions [66,76]. The proximity of the opaque white layers to, respectively, red and blue layers could have promoted the formation of this mineral.

Although calcium antimoniate was not detected in the analyzed samples, this compound was observed in contemporaneous glass fragments in two *millefiori* glass samples found in the SCV context with an attributed genuine Venetian production [20] and in a genuine Venetian glass goblet with a *splashed* decoration [52]. This observation provides evidence that during the Renaissance period, although antimony components seemed to be favored as an opacifier among Venetian glassmakers, they were still using tin in the production of coeval glass objects.

3.4. Morphological Characterization of Millefiori Fragments

While only 15 *millefiori* glass fragments from the SCV archeological site plus 2 *millefiori* glass fragments found in the SJT context were selected to be analyzed, the morphological characterization will include the total of the entire *millefiori* glasses of the SCV assemblage that were previously studied [7], which means that 276 more fragments will be included. Considering the SCV and SJT contexts, at least 31 *millefiori* glass objects were calculated [7].

The identification of the *murrina* original patterns can be a challenge because the fragment can be too degraded (e.g., SCV_222 and SCV_389 fragments in Figure 19) or the sliced cane can appear rolled (e.g., SCV_232 fragment in Figure 19) due to the production process of *millefiori* glass (consult [1], p. 6 for a deeper understanding of how to produce *millefiori* glass). These unidentified patterns were considered as "undetermined" in the classification.

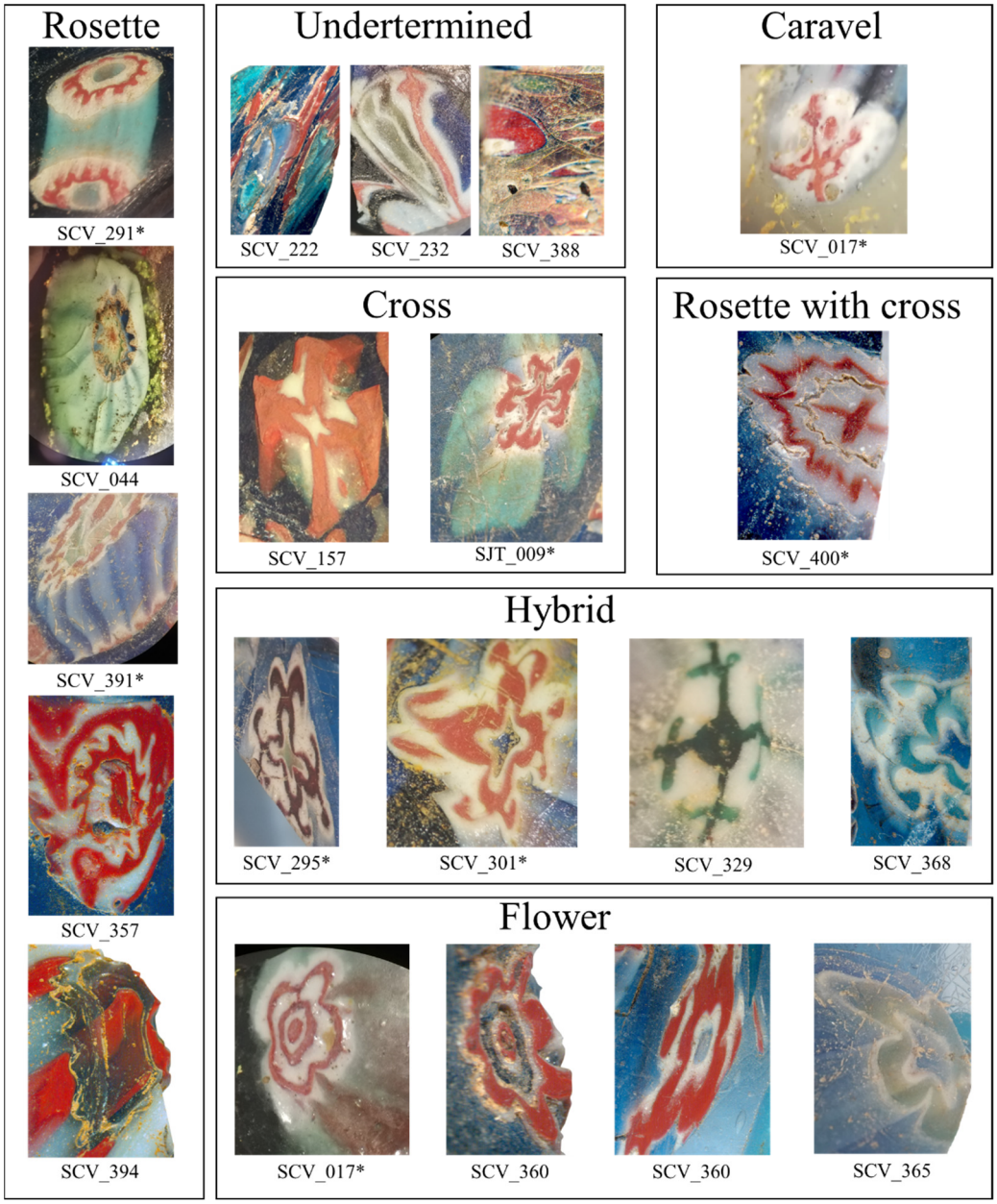

Figure 19. Images of the different groups of decoration patterns belonging to the *millefiori* glass fragments found in the SCV and SJT contexts (* represent the glass fragments that were not compositionally analyzed).

The study of the different glass patterns of the *millefiori* fragments gathered from the SCV and SJT contexts will be discussed according to its abundance based on the estimated glass objects.

The different patterns identified in the samples are divided in *flower*, *rosette*, *caravel*, *cross*, *rosette with cross*, *and hybrid* (Figure 19).

The observed frequency of the different patterns is in accordance with P. Hollister's [77] investigations, apart from the "*undetermined*" group, that gathers more than 40% of the patterns (18 out of 44); the "*rosette*" pattern is the most popular with a representativity of more than 25% (11 out of 44) with or without a cross in the core. This value is followed by the "*hybrid*" (4 out of 44), "*flower*" (3 out of 44), and "*cross*" patterns (2 out of 44).

The less common "*caravel*" pattern detected twice in the SCV_017 glass fragment (1 out of 44) was also observed in a glass fragment found in the Santana Convent (Lisbon) [18]. Although this sample was not analyzed in this study, this is considered to be a remarkable finding, as *caravels* and the *cross of Christ* have a huge importance in the Portuguese identity of the 17th century. They represent the Portuguese expansions, one of the main objectives of which was evangelism. The cross of Christ, also known as cross of Portugal (Figure 19, SJT_009 fragment), was the symbol used by the military Order of Christ, inheriting the knowledge and the patrimony of the Order of Templars dissolved by Pope Clement V in 1312 [29]. This cross was used in the coeval Portuguese caravel sails, coins, and as architectural ornaments, but it is still in use today by entities such as the Portuguese Air Force in the aircrafts and in the Portuguese Navy ships.

Although no parallel with our *flowers* or *hybrid* (half a cross/half a flower) patterns were discovered in *millefiori* glass objects/fragments outside Portugal [1], these decorative patterns were profusely used as architectural ornaments whether in Portugal or abroad.

Also, it is interesting to point out that two canes were also detected in the SCV context (Figure 20). Can these fragments be viewed as a consequence of glass working? Can SCV_366 be used in the *murrine* of the SCV_368 sample (Figure 19)?

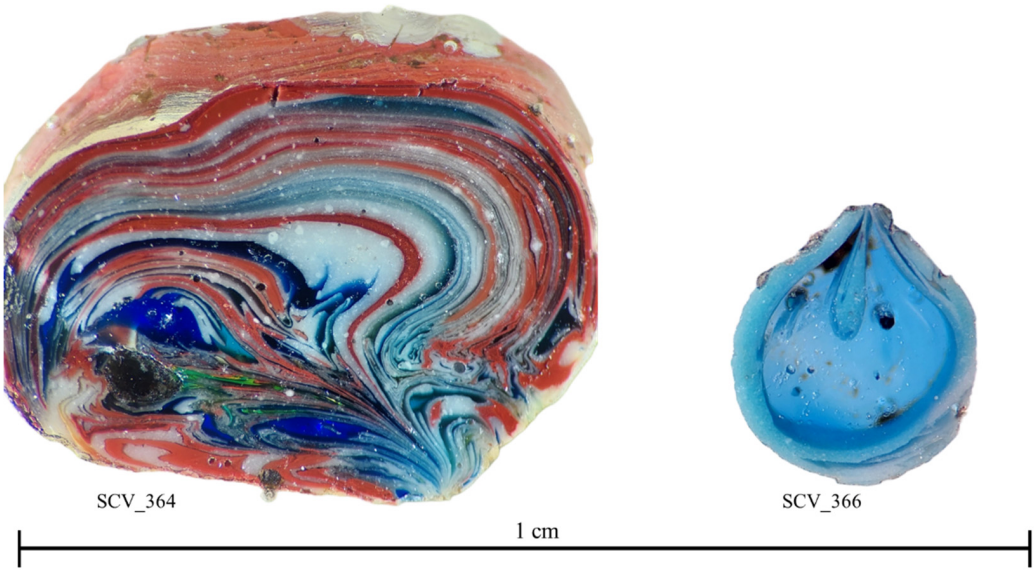

Figure 20. Image of the cross-section of the SCV_364 and SCV_366 glass canes.

3.5. Summary

All the studied colored glass layers are in accordance with contemporary glass compositions reported in the literature for Venetian and *façon-de-Venise* glass of the 17th century.

Although all the 76 analyzed glass layers can be considered to be of the soda–lime–silica type (the most used in Venetian and *façon-de-Venise* glass artifacts), different groups of alkali sources were detected: 44% (33 out of 76) were considered a mixture of halophytic plant ashes, 36% (27 out of 76) fall in the *façon-de-Venise* region of the graph (Figure 4), and

only 20% (15 out of 76) were made by using Levantine ashes, of which only half (7 glass layers) were purified.

This result (20% of *Levantine* ashes) is surprisingly low because *millefiori* glass is usually attributed to a Venetian production, and Venetian glass makers were only allowed to use the best raw materials in the finest objects. This evidence opened some questions, like:

- Could it be that this is true for colorless glass but does not apply to colored glass, since a greenish tint may not have much influence on the final color of cobalt blue or copper red, for instance? The truth is that purified Levantine ashes were detected in clear (3 layers), blue- (2 layers), and white (2 layers)-colored glass and in clear (2 layers), blue- (2 layers), red- (2 layers), turquoise- (1 layer), and white (1 layer)-colored glass made with unpurified Levantine ashes (Table 4).

Considering the oxides related to silica sources and comparing our results with the reported information gathered from the literature, only 4 layers belong to Venetian production; another 4 are placed in the Two Roses, a Dutch glasshouse; and 15 glass layers fall between the Venetian and Two Roses regions of the graph (Figure 5 and Table 4). The Granada region of the graph is represented by 2 glass layers plus 2 glass layers that fall between Granada and Two Roses. The proposed Lisbon area is represented by almost 60% (39 fall in the Lisbon region and 6 nearby, giving in total, 45 samples) of the analyzed glass layers (Figure 5 and Table 4).

By the normalization of trace and REEs to Earth's upper crust, four different geochemical patterns were detected (Figure 7), which can indicate that four different geochemical settings were used in the glass production of these glass fragments. Gathering all the information presented in this section, it is interesting to note that some samples where Levantine ashes were used cannot be considered Venetian production due to its high amount of titanium and alumina oxides (**SCV_044cl**/**SCV_046cl**/SCV_250b/**SCV_272cl**/**SCV_275cl**/**SCV_365b**/SCV_365w/**SCV_368b**/SCV_368w/SCV_388w/**SCV_394cl**, the highlighted samples belong to the glass body).

In the samples that have some glass layers compatible with Venetian production, according to the amount of alkali and silica sources (SCV_235r/SCV_250b/SCV_250t/SCV_275r/SCV_366b/SCV_394b), they belong to the PG4.

Surprisingly, none of the analyzed fragments can be attributed to Venetian production, as the composition of only a few layers match with the values reported in the literature for Venetian glass artifacts. In addition, some glass layers, which are comparable to Venetian production, do not belong to the finest fragments, such as the *splashed* fragments displaying a yellowish glass body (SCV_235r/SCV_275r) and one layer of the *murrine* cane (SCV_366b). Moreover, although the glass body of the SCV_250 fragment is incredibly transparent, the decorative patterns of this sample and of the SCV_394 sample are not very detailed (Table 4).

Three glass layers (SCV_216w, **SCV_360b**, and SCV_360b) have compositions of alkali and silica sources that are compatible with the Dutch production, here represented by the Two Roses glasshouse [51]. However, for these layers, two different GPs were detected: 2 and 3 (Table 4). In the same sample, SCV_360 displays an amazing and detailed flower and hybrid decorative patterns (Figures 2 and 19), and, in all the other glass layers, the detected GP is the GP3 (Table 4), which was suggested to have a Lisbon attribution [18] due to the compatibility of 8 *pick-up* glass fragments and 4 glass production remains, which were found in two different archeological contexts in Lisbon where this geochemical pattern was detected for the first time.

Regarding the samples that have a glass body that does not match with all or a part of the *murrine*'s layers (e.g., SCV_216 or SCV_235), this observation can be considered an indication that different glass origins and/or different glass recipes were combined to create the intricate designs that can be observed in the considered *pick-up* glass objects. Different glass recipes applied to the glass body and the different layers of *murrine* were also previously noted by Augusta Lima [20] for some SCV *millefiori* glass fragments from the SCV context and by Verità and Zecchin [52] on a Venetian *splashed* glass goblet dated to the 16th Century.

The GP1 was only found in the SCV_365 and SCV_368 glass bodies and white layers. This glass is comparable with the production remains found in Granada [10], regarding the alkali and silica sources (Table 4). Can this observation indicate that these fragments have a Spanish origin? Although further analyses must be conducted to propose a Spanish/Iberian origin for these fragments, this is an interesting result that cannot be overlooked.

GP2 was only detected in all glass layers belonging to SCV_216 and SCV_388, as well as in 5 other glass layers (Table 4). Yet, this GP is not associated with any glass production center, and no specific morphological characteristics were detected.

GP3 represents about 41% (30 out of 73) of total analyzed layers and was only detected in the SCV assemblage. This pattern is represented in all layers of 7 fragments (SCV_044/SCV_245/SCV_275/SCV_357/SCV_360/SCV_369/SCV_375) that display a wide range of quality regarding the color choice of the glass body (blue, clear, grayish, and yellowish) and decorative motives (from undetailed, decorative patterns like the SCV_044 fragment to a more detailed pattern like the SCV_360 fragments).

In addition, this GP was also detected in the glass body of other samples, such as SCV_235, SCV_236, SCV_250, SCV_329, and SCV_394. This result can mean that while the different colored glass layers belonging to the *murrine* of these last fragments can be imported from other glass production centers, the objects were made in the same production center of, e.g., SCV_044 and SCV_360 samples or, at least, by using the same/related geological silica source.

This GP was detected in some glass slags found in Lisbon which match with some *filigrana* and *pick-up* glass fragments found in this city and in some gourd-shaped vessels. Based on this evidence, and due to no known foreign parallel being reported in the consulted literature, we are able to propose that GP3 may be linked to a Portuguese production, as suggested in previous studies [1].

GP4 is the second-most-abundant GP, representing more than 37% of the total analyzed glass layers (27 out of 73). It is composed of fragments found in both contexts (SCV and SJT) and is present in all the analyzed layers of SCV_232, SCV_364, SCV_366, and SJT_001 fragments (Table 4). Interesting to note is that, both the SCV_366 and SJT_001 fragments have a high quality regarding the detailed decorative pattern.

Gathering all the information we obtained about silica sources reported in Table 4 (major components, GP and Eu/Eu*), it is interesting to note that only the GP4 can be associated with Venetian production. This observation allows us to propose that GP4 is maybe linked with Venetian production.

Other information that must be discussed here is the SJT_009 glass fragment that presents the important symbol of the cross of Christ. In this fragment, GP4 was detected in all the analyzed glass layers. However, the amount of alumina (higher than 2 wt%) is not consistent with the values attributed to Venetian production. To our knowledge, no parallels regarding this geochemical pattern is known, so the attribution to Venetian production cannot be made for this glass artifact.

Interesting to point out is that, for the natural greenish glass body of SCV_046 fragment that present a *gourd shape*, the GP4 was detected (Figure 7). As the gourd shape has been attributed to Portuguese production [17], this geochemical pattern can also perhaps be linked to a Portuguese origin. Beyond the gourd-shaped vessel, some layers belonging to SCV_232 (Body, r, w) and SCV_394 (r, w) fragments that present some undefined *rosette* pattern were also detected. Moreover, parts of the SCV_364 (r, t, w) *murrine* cane and the yellowish glass body of SCV_272 fragment also present the GP4 characteristics. All these fragments seem to have less quality when compared with other fragments like SCV_360, SCV_368, or SJT_009. This observation suggests that it is quite difficult to make a Venetian attribution as coeval Venetian glass objects are well known by their high quality and perfection.

Considering the glass chromophores presented in colored glass, some observations can be noted:

- **Blue** is mainly influenced by Co^{2+}, while Cu^{2+}, $Fe^{2+/3+}$, and MnO were also detected in some samples.
- **Green** is produced due to an equilibrium between Fe^{2+} and Fe^{3+} ions.
- **Purple** was only observed once (SCV_368 sample), and Co^{2+} and MnO contributed to the final color.
- **Red** was formed under reduced conditions which favored the development of cupper nanoparticles of Cu^0 and Cu_2O dispersed in the glass matrix.
- **Turquoise** was achieved in an oxidizing environment which favored the development of Cu^{2+} ions.
- **White** glass layers were obtained by the addition of lead and tin oxides to the base glass, favoring the growing of cassiterite and malayaite crystals.

4. Conclusions and Future Work

The studied *pick-up* glass fragments were selected according to their representativity, considering the range of colors, different decorative patterns, and the shape of the original object.

All the analyzed glass layers are of soda–lime–silica type, a composition that is in accordance with what is expected for historical glass dated to the 17th century.

The alkali source used in theses samples were halophytic plant ashes (plants that grow in arid regions or near the sea and have a high sodium content). They were divided into different groups, with the composition related to the alkali sources compatible with the addition of the following: (1) purified Levantine ashes; (2) unpurified Levantine ashes; (3) Façon-de-Venise, which is usually attributed to barilla plant ashes; and (4) a mixture of ashes (or a semi-purification process).

On the other hand, the data related to the silica source shows high dispersion (Figure 5). While the SJT samples are in the Lisbon area or nearby, SCV glass layers are dispersed throughout the chart, which is related to the diverse mineralogy of the glassmaking sands. This was confirmed by the detection of 4 different GPs.

Apart from GP4, which is present in both contexts, the remaining were detected only in the SCV glass fragments.

The heterogeneity of the SCV assemblage can be linked to the historical importance of this site, as it was here that the only Queen declared a saint by the Catholic church wanted to be entombed. Her canonization happened in 1625; this event must have attracted many pilgrims who potentially donated objects to pay for their promises. In addition, we know that the wealthiest nuns belonging to the noble families and upper bourgeoisie brought their personal and luxurious belongings when they joined this monastery. It is worth noting that, according to historical documentation, at least one glass furnace was working near the convent [31].

GP1 was associated with the data reported for the Granada furnace, with regard to the major elements associated with silica sources (SiO_2, Al_2O_3, and TiO_2). Two glass samples from the SCV (SCV_365 and SCV_368) contexts presented these characteristics.

GP2 was only detected in 16% of the analyzed glass layers, and no parallels were found.

The most detected GP in this study was the GP3. This pattern represented about 41% of the total analyzed glass layers and was linked to some glass slags and *pick-up* glass fragments found in two different archeological contexts located in Lisbon. The glass fragments belonging to GP3 were dispersed by all the different areas of the alkali sources graph (Figure 4). Looking to the major oxides associated with silica sources (SiO_2, TiO_2, and Al_2O_3), we could conclude that, while the glass layers are dispersed throughout the graph, more than 80% of the glass layers belonging to PG3 fall in the Lisbon region or nearby. This result can suggest that these fragments may have a Portuguese origin.

Here, it is important to mention that while historical documentation suggests that some Portuguese glass productions attained a level of quality comparable to Venetian

production, the absence of archeological evidence regarding the production furnaces and associated artifacts hinders a definitive attribution of GP3 to Portuguese glass production.

The second most popular GP belongs to the GP4. This group is composed of glass fragments of both archeological contexts (SCV and SJT), and, while no parallel for this pattern was found, it is interesting to note that more that 22% of these layers can be considered of Venetian production according to the main oxides attributed to silica sources (SiO_2, Al_2O_3, and TiO_2). In this group is also one of the most important glass objects studied in this project—the SJT_009 fragment—because of the huge symbolical meaning for the Portuguese identity of the decorative pattern: the cross of Christ, also known as the cross of Portugal. This decorative pattern does not have any parallel outside, but the Venetian attribution was discarded due to its high alumina values (higher than 2%).

In GP4, a possible Portuguese production was also pointed out due to the greenish glass body of the gourd-shaped SCV_046 fragment, which has been attributed Portuguese origin.

In addition, more data related with trace and rare earth elements taken form glass fragments/objects of this historical period are needed to propose more accurate conclusions. To our knowledge, the data related with titanium oxide and GP are limited for the main glass production centers (Venice, Bohemia, France, Low Countries, England, or the Iberian Peninsula) of the Modern period. More attention needs to be paid to these glass objects in order to better value and preserve them.

Supplementary Materials: The following supporting information can be downloaded at: https://www.mdpi.com/article/10.3390/heritage7090239/s1, Table S1: Information about the archaeological context and the distribution of the glass fragments decorated with pick-up technique; Table S2: Presentation of the glass composition for the glass material used for the calibration of LA-ICP-MS equipment (N610, N612, CORNA, CORNB, CORND and CORNC). The composition is presented in average (wt% for oxides and μg/g for the elements) as well as the relative standart deviations (RSD) for each referenced glass.; Table S3: Composition of the clear and colored glass (in wt%) calculated by subtracting the colorants, opacifiers and correlated elements and then normalizing it to 100%. All the presented values were acquired through LA-ICP-MS analyses Table S4: Composition of the analysed production waste and millefiori glass fragments unearth in Lisbon determined by LA-ICP-MS in weight percent of oxides up to iron oxide and in μg/g for all the remaining oxides. The chemical composition of red and clear glass presented in body glass of LCS_05 are highlighted. All the presented values were acquired through LA-ICP-MS anal-yses.

Author Contributions: For this article, all the authors contributed substantially: Conceptualization, F.P.V. and M.V.; methodology, F.P.V. and I.C.; software, B.G. and L.C.A.; validation, A.C., F.P.V., I.C. and T.M.; formal analysis, B.G. and L.C.A.; investigation, F.P.V., I.C., T.M. and M.V.; resources, F.P.V.; data curation, F.P.V.; writing—original draft preparation, F.P.V.; writing—review and editing, A.C., I.C., T.M., L.C.A., B.G. and M.V.; visualization, F.P.V.; supervision, M.V., I.C. and T.M.; project administration, M.V.; funding acquisition, M.V. and F.P.V. All authors have read and agreed to the published version of the manuscript.

Funding: This project was supported by the Portuguese Science and Technology Foundation (FCT-MCTES), grants: PD/BD/114407/2016, UID/00729/2020.

Data Availability Statement: Data are contained within the article and Supplementary Materials.

Acknowledgments: The authors are very grateful to the Lídia Fernandes and António Valongo; to Helena Catarino; to the direction bodies from the archeological company Crivarque, Mosteiro de Santa Clara-a-Velha, and Mosteiro de São João de Tarouca, who provided access to their glass assemblages, giving opportunity for this work to be realized; and to the unknown reviewers of this paper, for their corrections, suggestions, and comments. Their work increases the value of this publication.

Conflicts of Interest: The authors declare no conflicts of interest.

References

1. Pulido Valente, F.; Coutinho, I.; Medici, T.; Vilarigues, M. Glass colored by glass: Review of the pick-up decoration in early modern Europe. *J. Archaeol. Sci. Rep.* **2021**, *36*, 102832. [CrossRef]
2. Wood, P. The tradition from Medieval to Renaissance. In *The History of Glass*; Klein, D., Lloyd, W., Eds.; LITTLE, Brown and Company: London, UK, 2000; pp. 67–91.
3. Baumgartner, E. Gobelets "a *millefiori* a" croix de malte. In *Bernard Perrot (1640–1709): Secrets et Chefs-D'oeuvre des Verreries Royales d'Orléans*; Somogy Editions' D'Art, Publications du Vitrocentre Romont (Bern: Lang), 2010; pp. 67–77.
4. Whitehouse, D. Renaissance and Modern Europe 1450-1900. In *Glass, a Short History*; Whitehouse, D., Ed.; The British Museum in Association with the Corning Museum of Glass: Corning, NY, USA, 2012; pp. 65–86.
5. Moretti, C. Vetro Mosaico, millefiori, murrine. *Boll. dei Civ. Musei Veneziani d'Arte e di Stor.* **1985**, *29*, 5–21.
6. Spenlé, V. Venezianische glas in Fürstlichen Kunst- und wunderkammern des 16. Und 17. Jahrhunderts/Venetian Glass in the 16th and 17th century princely Kunstand Wunderkammer. In *The White Gold of Venice*; Laue, G., Ed.; Filigree Glass for European Kunstkammer; Kunstkammer Georg Laue: München, Germany, 2014; pp. 40–65.
7. Medici, T. Vidros da Terra. O vidro tardomedieval e moderno em Portugal (séculos XIV-XVII). O Contributo da Arqueologia. A Thesis Submitted in Fulfilment of the Requirements of Universidade de Coimbra for the Degree of Doctor of Archaeology. Faculdade de Letras da Universidade de Coimbra. 2014. Available online: https://estudogeral.sib.uc.pt/handle/10316/26739 (accessed on 10 September 2024).
8. Amado Mendes, J. *Hitória Do Vidro e Do Cristal em Portugal*; Edições Inapa: Lisbon, Portugal, 2002.
9. Valente, V. *O Vidro em Portugal*; Portucalense Editora: Porto, Portugal, 1950.
10. Coutinho, I.; Cambil Campaña, I.; Alves, L.C.; Medici, T. Callen horno del vidrio–preliminary study of glass production remains found in Granada, Spain, dated to the 16th and 17th centuries. *Minerals* **2021**, *11*, 688. [CrossRef]
11. Baart, J.M. The façon de Venise glass of Amsterdam. In *Majolica and Glass: From Italy to Antwerp and Beyond. The Transfer of Technology in the 16th–early 17th Century*; Veeckman, J., Ed.; Stad Antwerpen: Antwerpen, Belgium, 2002; pp. 161–171.
12. Gawronski, J.; Hulst, M.; Jayasena, R.; Veerkamp, J. Glasafval op het achtererf, AAR50 (Amsterdamse Archeologische Rapporten). 2010. Available online: https://www.academia.edu/5915086/Glasafval_op_het_achtererf_Amsterdamse_Archeologische_rapporten_50 (accessed on 10 September 2024).
13. Henkes, H.E. Glas zonders glans. Vijf gebruicksglas uit de bodem van de Lage Landen 1300–1800/Glass without gloss. In *Utility Glass from Five Centuries Excavated in the Low Country 1300–1800*; Coördinatie Commissie van Advies Inzake Archeologisch Onderzoek Binnen Het Ressort: Rotterdam, The Netherlands, 1994.
14. Hulst, M. In de zeventiende eeuw was Amsterdam een belangrijk productiecentrum van kleurloos luxe glaswerk, het façon de Venise. Hoewel in Netherland opgegraven façon de Venise steevast aan Amsterdamse glasovens wordt toegeschreven, bleef de identificatie ervan tot voor kort onzeker. In *Glazen Met Maskerons en Leeuwenkopstammen uit Amsterdamse Bodem. Een Aanzet tot de Identificatie van Zeventiende-Eeuwse Amsterdamse Façon de Venise*; 2013; pp. 21–38. Available online: https://www.academia.edu/5881032/Glazen_met_maskerons_en_leeuwenkopstammen_uit_Amsterdamse_bodem (accessed on 10 September 2024).
15. Dungworth, D.; Cromwell, T.; Ashurst, D.; Cumberpatch, C.; Higgins, D.; Willmott, H. Glass and pottery manufacture at Silkstone Yorkshire. *Post-Medieval Archaeol.* **2006**, *40*, 160–190. [CrossRef]
16. Barosa, J.P. Fabrico do Vidro e Vidreiros de Portugal: Do século XV ao Longo do Século XVII (1438–1714). 2022. Available online: https://www.researchgate.net/publication/361665458_Fabrico_do_Vidro_e_Vidreiros_em_Portugal_ca_1439_-_1714 (accessed on 10 September 2024).
17. Coutinho, I.; Medici, T.; Wiley, R.; Alves, L.C.; Gratuze, B.; Vilarigues, M. The Gourd-Shaped Vessel: A Portuguese Product? *J. Glass Stud.* **2017**, *59*, 215–234.
18. Pulido Valente, F.; Coutinho, I.; Medici, T.; Gratuze, B.; Alves, L.C.; Varela Gomes, R.; Varela Gomes, M.; Vilarigues, M. In the quest for historical Lisbon through 17th century Millefiori glass. *J. Archaeol. Sci. Rep.* **2023**, *52*, 104228. [CrossRef]
19. Pulido Valente, F.; Varela Gomes, R.; Varela Gomes, M.; Coutinho, I.; Medici, T.; Vilarigues, M. Renaissance millefiori glass: The Portuguese case study. In *Interim Meeting of ICOM-CC, Glass and Ceramics Working Group*; Conference Proceedings; Mandrus, J., Schussler, V., Eds.; ICOM: London, UK, 2019; pp. 217–221.
20. Lima, A.; Medici, T.; Pires de Matos, A.; Verità, M. Chemical analysis of 17th century Millefiori glasses excavated in the Monastery of Sta. Clara-a-Velha, Portugal: Comparison with Venetian and façon-de-Venise production. *J. Archaeol. Sci.* **2012**, *39*, 1238–1248. [CrossRef]
21. Coutinho, I.; Medici, T.; Alves, L.C.; Gratuze, B.; Vilarigues, M. Provenance studies on façonde-de-Venise glass excavated in Portugal. *J. Archaeol. Sci. Rep.* **2016**, *7*, 437–448. [CrossRef]
22. Varela, M.R. Estudos de Proveniência de um Conjunto de Vidros Filigranados Datados dos Séculos XVI–XVII Encontrados no Largo do Chafariz de Dentro, Lisboa. Master's Thesis, Faculdade de Ciências e Tecnologia, Universidade Nova de Lisboa, Monte de Caparica, Portugal, 2018. Available online: https://run.unl.pt/bitstream/10362/68861/1/Varela_2018.pdf (accessed on 10 September 2024).

23. Trindade, S.D.; Gambini, L.I. *Mosteiro de Santa Clara de Coimbra: Do Convento à Ruína, da Ruína à Contemporaneidade. Côrte-Real, Artur (coord.)*, 2nd ed.; Direção Regional da Cultura do Centro: Coimbra, Portugal, 2009. Available online: https://www.academia.edu/21876251/Mosteiro_de_Santa_Clara_de_Coimbra_do_convento_%C3%A0_ru%C3%ADna_da_ru%C3%ADna_%C3%A0_contemporaneidade (accessed on 10 September 2024).
24. Varela Gomes, M.; Varela Gomes, R.; Casimiro, T.M. Convents, monasteries and porcelains: A case study of Santana Convent, Lisbon. In *Global Pottery Proceedins–1st International Conference for Historical Archaeological and Archaeometry for Societies in Contact*; Garrigós, J.B., Fernández, M.M., Iñañez, J.G., Eds.; BAR International Series; Archaeopress: Oxford, UK, 2015; Volume 2761, pp. 93–101.
25. Barroso Catalão, S. *Mosteiro de São João de Tarouca e a Arqueologia da Arquitectur: O «Aljube». Museu de Lamego, Direcção Regional da Cultura do Norte*; 2018; ISBN 978-989-99516-5-5. Available online: https://issuu.com/066239/docs/msjt_aljube_catalaosofia2018 (accessed on 10 September 2024).
26. Sampaio e Castro, A.; Sebastian, L. *Imtervenção Arqueológicano no Mosteiro de São João de Tarouca: 1998–2001*; Estudos: Património, Estudos/Património; IPPAR—Departamento de Estudos: Lisboa, Portugal, 2002; n.º 2; pp. 33–42.
27. Bellanger, J.; de Venise, L.P.; Massin, C. (Eds.) *Histoire du Verre, L'Aube des Temps Modernes: 1453–1672*, 1st ed.; Massin Editor: Reims, France, 2006; Volume 3, pp. 25–28. Available online: https://www.amazon.fr/Histoire-verre-Laube-modernes-1453-1672/dp/2707205214 (accessed on 10 September 2024).
28. Albuquerque Carreira, J. Cister, os Templários e a Ordem de Cristo. In *I Colóquio Internacional*; Albuquerque Carreira, J., Rossi Vairo, G., Eds.; Instituto Politécnico de Tomar: Tomar, Portugal, 2012; pp. 21–30.
29. Vasconcelos, M.A.; Mantero, I. *A Monarquia Portuguesa: Reis e Rainhas na História de um Povo*; Selecções do Reader's Digest: Lisbon, Portugal, 1999; ISBN 972-609-261-2.
30. Fernandes, A. Iluminando o Passado: Estudos do Conjunto de Lamparinas em Vidro do Mosteiro de São João de Tarouca, séculos XVII–XVIII. NOVA Doctoral School of Science and Technology. Master Dissertation, Universidade NOVA de Lisboa, Lisbon, Portugal, 2020. Available online: https://run.unl.pt/bitstream/10362/158344/1/Fernandes_2021.pdf (accessed on 10 September 2024).
31. Ferreira, M. Espólio vítreo proveniente da estação arqueológica do Mosteiro de Sta. Clara-a-Velha de Coimbra: Resultados preliminares. *Rev. Port. Arqueol.* **2004**, *7*, 541–583.
32. Medici, T. *Revisiting the "Moura Glass Treasure": New Data about 17th Century Glass in Portugal*; Annales du 18e Congrès de l'Association Internationale pour l'Histoire du Verre (AIHV): Thessaloniki, Greece, 2012; 442–447.
33. Pulido Valente, F.; Coutinho, I.; Vilarigues, M.; Medici, T. A 16th–17th Century Filigrana glass found in Portugal: Some preliminary observations. In Proceedings of the Study days on Venetian Glass, Venetian Filigrana Glass through the Centuries, Venice, Italy, 11–13 September 2017; ATTI, Classe di scienze fisiche, matematiche e naturali. 2018; Volume 176, pp. 139–152.
34. Gratuze, B. Glass characterization using Laser Ablation Inductively Coupled Plasma Mass Spectrometry. In *Mothern Methods for Analysing Archaeological and Historical Glass*; Janssens, K., Ed.; Wiley: Chichester, UK, 2013; pp. 200–234.
35. Gratuze, B. Glass characterization using Laser-Ablation-Inductively Coupled Plasm-Mass Spectroscopy method. In *Recent Advances in Laser Ablation ICP-MS for Archaeology (coll. Natural Sciences in Archaeology)*; Dussubieux, L., Golitko, M., Gratuze, B., Eds.; Springer: Berlin/Heidelberg, Germany, 2016; pp. 602–613.
36. Biron, I.; Veritá, M. Analytical investigation on Renaissance Venetian enamelled glasses from the Louvre collections. *J. Archael. Sci.* **2012**, *38*, 2706–2713. [CrossRef]
37. Thornton, D.; Freestone, I.; Gudenrath, W.; Bertini, M.; Meek, A.; Ling, D. The technical study of a rare Venetian turquoise glass goblet from the Waddesdon Bequest. In *British Museum Technical Research Bulletin*; The British Museum: London, UK, 2014; Volume 8, pp. 1–11.
38. Cagno, S.; Brondi Badano, M.; Mathis, F.; Strivay, D.; Janssens, K. Study of glass fragments from Savona (Italy) and their relation with the glass produced in Altare. *J. Archaeol. Sci.* **2012**, *39*, 2191–2197. [CrossRef]
39. Janssens, K.H.; De Raedt, I.; Schalm, O.; Veeckman, J. Composition of 15-17th century archaeological glass vessels excavated in Antwerp, Belgium. *Mikrochim. Acta [Suppl.]* **1998**, *15*, 253–267.
40. Wouters, H.; Fontaine, C. The large Catalonian Ewer from the Glass Museum of Liège (Second Half of the 16th Century–Beginning of the 17th Century): Restauration and Scientific Analysis. In Proceedings of the Annales du 17e Congrès de l'Association Internationale pour l'Histoire Du Verre (AIHV), Antwerp, Belgium, 4–8 September 2006; pp. 408–413.
41. Cagno, S.; De Raedt, I.; Jeffries, T.; Janssens, K. *Composition of Façon-de-Venise Glass from Early 17th Century London in Comparison with Luxury Glass of the Same Age*; Integrated Approaches to the Study of Historical Glass: Brussels, Belgium, 2012; p. 842205. [CrossRef]
42. Verità, M. Venetian soda glass. In *Modern Methods for Analysing Archaeological and Historical Glass, Vol. I*; Janssens, K., Ed.; Wiley: Chichester, UK, 2013; pp. 515–536.
43. Verità, M.; Toninato, T. *A Comparative Analytical Investigation on the Origins of the Venetian Glassmaking*; Rivista della Stazione Sperimentale del Vetro 4: Venezia, Italy, 1990.
44. Moretti, C.; Hreglich, S. Raw materials, recipes and procedures used for glass making. In *Modern Methods for Analysing Archaeological and Historical Glass*; Janssens, K., Ed.; John Wiley & Sons: Hoboken, NJ, USA, 2013.
45. Verità, M. *L'invenzione del Cristallo Muranese: Una Verifica Analitica Delle Fonti Storiche*; Rivista della Stazione Sperimentale del Vetro 1: Venezia, Italy, 1985; pp. 17–29.

46. Verità, M.; Zecchin, S. Thousand years of venetian glass: The evolution of chemical composition from the origins to the 18th century. In *Annales de l'Association Internationale pour l'Histoire du Verre 17, Antwerp 2006*; Janssens, K., Degryse, P., Cosyns, P., Caen, J., Vańt dack, I., Eds.; University Press Antwerp: Antwerp, Belgium, 2009; pp. 602–613.
47. De Raedt, I.; Janssens, K.; Veekman, J. On the distinction between 16th and 17th century Venetian and façon-de-venise glass. In *Majolica and Glass–from Italy to Antwerp and Beyond. The Transfer of Technology in the 16th–Early 17th Century, Antwerp*; Veeckman, J., Jennings, S., Dumortier, C., Whitehouse, D., Verhaeghe, F., Eds.; 2002; pp. 95–154.
48. Šmit, Ž.; Stamati, F.; Civic, N.; Vevecka-Priftaj, A.; Kos, M.; Jezersek, D. Analysis of Venetian-type glass fragments from the ancient city of Lezha (Albania). *Nucl. Instrum. Methods Phys. Res. B* **2009**, *267*, 2538–2544. [CrossRef]
49. Cagno, S.; Mendera, M.; Jeffries, T.; Janssens, K. Raw materials for medieval to post-medieval Tuscan glassmaking: New insight from LA-ICP-MS analyses. *J. Archaeol. Sci.* **2010**, *37*, 3030–3036. [CrossRef]
50. Schibille, N.; Sterrett-Krause, A.; Freestone, I.C. Glass groups, glass supply and recycling in late Roman Carthage. *Archaeol Anthropol Sci* **2017**, *9*, 1223–1224. [CrossRef]
51. Kunicki-Goldfinger, J.; Hulst, M. The golden age of Amsterdam glass. A chemical and typological approach to recognize Amsterdam 17th century glass production. In Proceedings of the Annales du 20e Congrès de l'Association Internationale pour l'Histoire du Verre (AIHV), Romont, Switzerland, 7–11 September 2015; pp. 547–553.
52. Verità, M.; Zecchin, S. Scientific investigation of a Venetian polychrome goblet of the 16th century. *J. Glass Stud.* **2008**, *50*, 97–104. Available online: https://www.jstor.org/stable/24191019 (accessed on 10 September 2024).
53. De Raedt, I.; Janssens, K.; Veekman, J.; Vincze, L.; Vekemans, B.; Jeffries, T.E. Trace analysis for distinguishing between Venetian and façon-de-Venise glass vessels of the 16th and 17th century. *J. Anal. At. Spectrom.* **2001**, *16*, 1012–1017. [CrossRef]
54. Lazar, I.; Willmott, H. The glass from the Gnalić wreck. In *Annales Mediterranea*; Koper, Slovenia, 2006; Available online: https://www.academia.edu/300405/The_Glass_from_the_Gnali%C4%87_Wreck (accessed on 10 September 2024).
55. Šmit, Ž.; Janssens, K.; Bulska, E.; Wagner, B.; Kos, M.; Lazar, I. Trace element fingerprinting of façon-de-Venise glass. *Nucl. Instrum. Methods Phys. Res. B* **2005**, *239*, 94–99. [CrossRef]
56. Brems, D.; Degryse, P. Trace element analysis in provenancing roman glassmaking. *Archaeometry* **2014**, *56*, 116–136. [CrossRef]
57. Costa, M.; Barrulas, P.; Dias, L.; Lopes, M.C.; Barreira, J.; Clist, B.; Karklins, K.; Jesus, M.P.; Silva Domingues, S.; Vandenabeele, P.; et al. Multi-analytical approach to the study of the European glass beads found in the tombs of Kulumbimbi (Mbanza Kongo, Angola). *Microchem. J.* **2019**, *149*, 103990. [CrossRef]
58. Costa, M.; Barrulas, P.; Dias, L.; Lopes, M.C.; Barreira, J.; Clist, B.; Karklins, K.; Jesus, M.P.; Silva Domingues, S.; Moens, L.; et al. Determining the provenance of the European glass beads of Lumbu (Mbanza Kongo, Angola). *Microchem. J.* **2020**, *154*, 104531. [CrossRef]
59. Wedepohl, K.H.; Simon, K.; Krons, A. Data on 61 chemical elements for the characterization of three major glass compositions in Late Antiquity and the Middle Ages. *Archaeometry* **2011**, *53*, 81–102. [CrossRef]
60. McDonough, W.F.; Sun, S.-S. The composition of the Earth. *Chem. Geol.* **1995**, *120*, 223–253. [CrossRef]
61. Kunicki-Goldfinger, J.; Pańczyk, E.; Dierżanowski, L.; Walliś, L. Trace element characterization of medieval and post-medieval glass objects by means of INAA and EPMA. *J. Radioanal. Nucl. Chem.* **2008**, *278*, 307–311. [CrossRef]
62. Coutinho, I.; Medici, T.; Gratuze, B.; Ruivo, A.; Dinis, P.; Lima, A.; Vilarigues, M. Sand and Pebbles: The Study of Portuguese Raw Materials for Provenance Archaeological Glass. *Minerals* **2022**, *12*, 193. [CrossRef]
63. Volf, M. Chemical approach to glass. In *Igneous Glassworks*; 2011.
64. Navarro, J.M.F. *El Vidrio, Colección Textos Universitarios, n○6*, 3rd ed.; Consejo Superior de Investigaciones Científicas Sociedad Española de Cerámica y Vidrio: Madrid, Spain, 2003.
65. Verità, M.; Zecchin, S.; Tesser, E. Venetian Filigree glass along the centu-ries: Some technological considerations. Study days on Venetian glass, Venetian filigrana glass through the Centuries. *ATTI Cl. Sci. Fis. Mat. Nat.* **2018**, *176*, 1–12.
66. Coentro, S.; Trindade, R.; Mirão, J.; Candeias, A.; Alves, L.C.; Silva, R.; Muralha, V.S.F. Hispano-Moresque ceramic tiles from the Monastery of Santa Clara-a-Velha (Coimbra, Portugal). *J. Archaeol. Sci.* **2014**, *41*, 21–28. [CrossRef]
67. Arletti, R.; Conte, S.; Vandini, M.; Fiori, C.; Bracci, M.; Porcinai, S. Florence baptistery: Chemical and mineralogical investigation of glass mosaic tesserae. *J. Archaeol. Sci.* **2011**, *38*, 79–88. [CrossRef]
68. Gratuze, B.; Soulier, I.; Blet, M.; Vallauri, L. De l'origine du cobalt: Du verre à la céramique. *Reveu D'archéométrie* **1996**, *20*, 77–94. [CrossRef]
69. Zucchiatti, A.; Bouquillon, A.; Katona, I.; D'Alessandro, A. The "Della Robbia blue": A case study for the use of cobalt pigments in ceramics during the Italian Renaissance. *Archaeometry* **2006**, *48*, 131–152. [CrossRef]
70. Bandiera, M.; Verità, M.; Patrice, L.; Vilarigues, M. The Technology of Copper Based Red Glass Sectilia from the 2nd Century AD Lucius Verus Villa in Rome. *Minerals* **2020**, *10*, 875. [CrossRef]
71. Moretti, C.; Gratuze, B. I vetri rossi al rame: Confronto di analisi e ricette. In Proceedings of the Annales du 14e Congrès de l'Association Internationale pour l'Histoire du Verre (AIHV), Venice-Milano, Italy, September 1998; pp. 227–232.
72. Loewen, B.; Dussubieux, L. The chemistry of Nueva Cadiz and associated beads: Technology and provenience. *BEADS J. Soc. Bead Res.* **2021**, *33*, 64–85. Available online: https://surface.syr.edu/beads/vol33/iss1/10 (accessed on 10 September 2024).
73. Veiga, J.P.; Figueiredo, M.O. Sixteenth century tubular glass beads: Nondestructive chemical characterization using synchrotron radiation XRF. *X-ray Spectrom.* **2002**, *31*, 300–304. [CrossRef]

74. Moretti, C.; Hreglich, S. *I Vetri Opachi. Sintesi Delle Tecniche Usate Dall'antichità all'Ottocento*; Atti delle IX Giornate Nazionali di Studio, Il vetro nell'Alto Adriatico: Venice, Italy, 2007; pp. 167–176.
75. Ricciardi, P.; Colomban, P.; Tournie, A.; Milande, V. Nondestructive on-site identification of ancient glass: Genuine artefacts, embellished pieces or forgeries? *J. Ranam Spectrosc.* **2008**, *40*, 604–617. [CrossRef]
76. Muralha, V.; Canaveira, S.; Mirão, J.; Coentro, S.; Morna, T.; Salerno, C. Baroque glass mosaics from the Capela de São João Baptista (Chapel of Saint John the Baptist, Lisbon): Unveiling the glassmaking records. *J. Raman Spectrosc.* **2015**, *46*, 483–492. [CrossRef]
77. Hollister, P. Muranese millefiori revival of the nineteenth century. *J. Glass. Stud.* **1983**, *25*, 201–206.

Tab. S1: Information about the archaeological context and the distribution of the glass fragments decorated with pick-up technique.

Countries	Cities	Contexts	Type	Date	Nº. frag.	Form	Dec. col.	Body col.	References
Autria	Tyrol	Medieval cemetery of the parish church of Innsbruck.	M	Before 1509	1	Millefiori bead	Ab, B, Bc, P, R, T	C	Personal information given by Mrs. Beatrix Nutz
Belgium	Antwerp	-	M	17th	1*	-	-	-	Henkes, 1994
Croatia	Gnalić	Gnalić wreck	S	16th-17th	2	Bottle and bowl	B, R, W	B	Lazar & Willmott 2006
			S	16th-17th	1	Bowl	B, R, W	R	
	Koločep	Koločep	S	17th	7	5 bowls, 1 vase and 1 jug	A, B, R	T	Medici 2010
			S	17th	3	2 bowls and tazza	A, B, R, T	W	
England	Coventry	Whitefriars	M	15th-16th	1*	Goblet	B, R, T, W	C	Willmott 2009
	London	Post Office Court	M	15th	2	Bowl	-	B	Charleston 1984; Tyson 1996; Willmott 2009
	Southampton	National Provincial Bank	M		1	Goblet	-	B	Charleston1984; Willmott 2009
	Yorshire	Silkstone (glass house)	S	17th	5	2 Beakers	W	Ab, B, C, Gn	Dungworth et al. 2006
France	Aveyron	*La Verrière* glasshouse	S	14th	6	-	B	G	Gratuze & Janssens 2004
	Orléans	-	M	16th	1*	Lid of a goblet	-	B	Barrera 1987; Page 2004
Hungary	Budapest	Buda Palace	M	15th	4*	Jars and chalices	-	-	Gerevich1952; Holl-Gyürky1986
Italy	Bormio	Piazza Cavour	M	15th-17th	2	Vessel	B, R, T, W	C	Uboldi 2015
	Ferrara	Sant' Antonio Monastery in Polesine	S	16th	1	Goblet	A, B, Bc, R, W	W	Verità & Zecchin 2008
	Gambassi	Piazza Del Castell	M	16th	6	-	-	-	Medici 2012; Mendera 2002
	Venice	Venetian Lagoon	M	15th	10	-	B, R, T, W	B/C	Moretti 2005; Verità 1985; Zecchin 1990a (1983)
Nether-lands	Amsterdam	-	S	17th	1	Beaker	-	C	Henkes, 1994
		Soop glasshouse	Both	17th-18th	1M + 4	Unknown	B, R, W	-	Baart 2002
		"De Twee Rozen" (The Two Roses)	Both	17th	1M + 3	Unknown	B, R, W, Y	B, C, Gn, W	Baart 2002, Gawronski et al. 2010
	Delft	-	M	17th	2*	Beakers	B, R, W	C	Henkes, 1994
	Leiden	-	M	17th	1*	-	-	-	Henkes, 1994

Tab. 1.2: Information about the archaeological context and the distribution of the glass fragments decorated with pick-up technique (Continued).

Countries	Cities	Contexts	Type of effect	Date	Nº. frag.	Form	Dec. col.	Body col.	literature
Portugal	Batalha	Santa Maria da Vitória Monastery	S	17th	1	Unknown	R,W	B	Teixeira 2014
	Coimbra	Santa Clara-a-Velha Monastery	Both	17th	220M + 81	Bottle/ Bowl/ Cup/ flask/ jug/ Vessel/ unknown	A, B, Gn, P, R, T, W	B, G, Gn, R, T, W	Ferreira 2004; Lima 2010; Lima et al. 2012; Medici 2014; Pulido Valente et al. 2017
	Lamego	São João de Tarouca Monastery	M	17th	2	Little flask, unknown	B, R, T, W	B	Medici 2014; Pulido Valente et al. 2017
	Lisbon	Largo do Chafariz de Dentro	M	16th-17th	1	Little bowl (M), unknown	B, R, T, W	B	Medici 2014; Pulido Valente et al. 2017
		Santana Convent	Both	16th-17th	9M +1	bird head, bottle, flask	B, R, T, W	B, C, G, R	Pulido Valente et al. 2017
	Moura	Santa Clara Convent	Both	17th	4M +1	Flask, gourd bottle shape	B, R, W	B	Medici 2012; Medici 2014; Pulido Valente et al. 2017
Slovenia	Ljubljana	Mengeš	M	16th	1*	Chalice	-	C	Kos 1994; Page 2004
Spain	Barcelona	Born	S	16th	2	1 Tazza	R, W	C	Beltrán de Heredia & Miró i Alaix 2006
						1 Cup	B	W	Beltrán de Heredia & Miró i Alaix 2006
	Granada	Alhambra	Both	17th	3M + 4	Little bottle	B, R, T, W	5 B, 2 C	Cambil & Sánchez 2016; Medici 2012
Syria	-	-	M	-	1	Sprinkler	-	-	Bruhn 1995
Switzerland	Bern	Waisenhausplatz	M	16th	3	Bowl (?)	B, R, T, W	C	Baumgartner 2015, p. 336

* When the author of the publication does not mention the number of fragments, was assumed that at least one or two, in the case that speaks in plural, exemplary were found.

Ab: Ambar; A: *aventurina*; B: blue; Bc: black; C: clear; G: grayish; Gn: Green; P: purple; R: red; T: turquoise; W= white; Y= yellow

M: millefiori

S: Splash

Nº. frag.: Number of considered fragments.

Dec. col.: Range of colours used in decoration.

Body col.: Body glass colour.

Tab. S2: Presentation of the glass composition for the glass material used for the calibration of LA-ICP-MS equipment (N610, N612, CORNA, CORNB, CORND and CORNC). The composition is presented in average (wt% for oxides and μg/g for the elements) as well as the relative standart deviations (RSD) for each referenced glass. (It is in the excel file entitled Tab_S2).

Tab. S3. Composition of the main components of clear glass and reduced compositions in wt% of the base glasses produced by subtracting the colorants, opacifiers and correlated elements and then normalizing it to 100%.

Sample	Color	Part	Na_2O	MgO	Al_2O_3	SiO_2	P_2O_5	Cl	K_2O	CaO	TiO_2
SCV_044	Blue	Cane	17.4	2.8	7.0	59.2	0.37	0.88	4.57	7.51	0.29
SCV_232		Body	11.0	3.1	2.1	67.8	0.27	0.72	4.77	10.17	0.07
SCV_245		Cane	15.5	3.3	4.4	60.9	0.34	0.77	5.60	8.98	0.19
SCV_250		Cane	14.5	3.6	1.5	66.8	0.31	0.90	2.22	10.18	0.06
SCV_329		Body	11.5	3.0	3.4	63.7	0.34	0.68	7.46	9.77	0.09
SCV_357		Body	18.7	3.1	4.1	31.3	0.32	1.11	3.55	7.62	0.14
SCV_360		Body	15.7	3.0	2.2	66.0	0.30	0.99	3.95	7.69	0.11
SCV_360		Cane	16.2	2.9	2.3	65.9	0.34	1.00	4.27	7.02	0.11
SCV_364		Cane	12.4	3.0	1.1	69.5	0.28	0.83	5.83	7.06	0.05
SCV_365		Body	17.6	2.0	3.4	66.9	0.43	1.10	3.83	4.53	0.23
SCV_365		Cane	16.3	2.7	3.3	65.5	0.46	0.93	3.91	6.80	0.15
SCV_366		Cane	13.0	3.6	1.2	70.0	0.22	0.72	2.30	8.93	0.07
SCV_368		Body	15.8	2.7	3.4	65.8	0.48	0.85	3.97	6.79	0.15
SCV_368		Cane	17.4	2.0	4.5	66.9	0.43	1.11	3.89	4.53	0.23
SCV_369		Body	18.0	3.1	4.1	61.1	0.35	1.03	4.79	7.32	0.16
SCV_369		Cane	17.7	3.2	4.2	61.1	0.33	1.00	4.76	7.47	0.16
SCV_375		Body	18.6	2.8	4.0	62.5	0.30	1.17	3.03	7.35	0.15
SCV_388		Body	18.8	2.9	3.9	62.5	0.37	1.19	3.32	6.87	0.18
SCV_394		Body	17.3	1.9	0.9	68.4	0.37	1.28	3.95	5.90	0.06
SJT_001		Body	12.7	3.6	4.4	59.1	0.42	0.69	7.34	11.52	0.14
SJT_009		Body	14.0	3.7	3.5	60.6	0.33	0.65	7.48	9.73	0.08
SCV_044	Clear	Body	21.3	2.9	7.2	58.7	0.35	1.19	4.19	3.87	0.34
SCV_046		Body	15.0	3.1	7.2	64.6	0.32	0.80	0.73	8.22	0.08
SVC_235		Body	14.9	3.0	3.6	64.3	0.23	0.70	5.13	8.01	0.18
SVC_236		Body	14.2	3.1	5.5	60.1	0.26	0.72	6.89	8.99	0.24
SVC_245		Body	15.6	3.6	4.8	60.3	0.35	0.86	5.68	8.63	0.21
SVC_250		Body	15.6	3.1	5.7	62.9	0.31	0.97	3.83	7.43	0.21
SCV_272		Body	19.1	7.1	7.7	57.0	0.84	0.99	1.89	5.09	0.30
SCV_275		Body	16.4	5.4	5.4	66.4	0.38	0.99	1.38	3.33	0.29
SCV_394		Cane	17.3	1.9	1.6	67.2	0.70	1.30	3.47	6.11	0.07
SCV_232	Green	Cane	11.1	3.2	2.2	66.7	0.26	0.85	5.01	10.48	0.08
SCV_368	Purple	Cane	15.9	2.7	3.4	65.8	0.48	0.88	3.92	6.74	0.15
SCV_044	Red	Cane	17.6	3.0	7.4	58.1	0.57	0.86	4.88	7.19	0.35
SCV_216		Cane	17.9	3.2	4.3	61.6	0.42	1.04	3.97	7.39	0.18
SCV_232		Cane	11.1	3.1	2.3	67.1	0.28	0.80	4.98	10.25	0.08
SCV_235		Cane	14.5	3.9	1.5	65.5	0.34	0.78	2.72	10.66	0.08
SCV_245		Cane	15.4	3.3	4.1	61.7	0.36	0.72	5.37	8.87	0.18
SCV_250		Cane	14.6	3.6	1.3	66.9	0.38	0.75	2.40	9.99	0.06
SCV_275		Cane	14.9	3.7	1.3	66.6	0.37	0.75	2.38	9.86	0.06
SCV_329		Cane	11.9	3.3	1.9	67.6	0.36	0.75	4.59	9.56	0.09
SCV_357		Cane	17.8	3.7	4.7	60.8	0.41	1.03	3.59	7.88	0.16
SCV_360		Cane	16.0	3.0	3.1	65.6	0.38	0.84	3.92	7.04	0.14
SCV_364		Cane	12.5	3.0	1.2	69.1	0.31	0.80	5.79	7.17	0.05
SCV_369		Cane	17.1	3.6	4.4	60.8	0.46	0.95	4.29	8.32	0.18
SCV_375		Cane	17.7	3.6	4.4	61.0	0.41	1.09	3.73	7.82	0.16
SCV_388		Cane	17.4	3.6	4.7	61.8	0.44	0.98	3.32	7.62	0.19
SCV_394		Cane	15.6	2.7	2.1	67.9	0.52	0.90	3.42	6.73	0.11
SJT_001		Cane	14.6	3.3	4.1	60.6	0.41	0.72	6.76	9.25	0.12
SJT_009		Cane	14.3	3.7	3.6	60.3	0.36	0.62	7.52	9.61	0.08

Tab. S3. Composition of the main components of clear glass and reduced compositions in wt% of the base glasses produced by subtracting the colorants, opacifiers and correlated elements and then normalizing it to 100% (Continued).

Sample	Color	Part	Na_2O	MgO	Al_2O_3	SiO_2	P_2O_5	Cl	K_2O	CaO	TiO_2
SCV_216	Turquoise	Body	15.0	3.5	2.5	65.5	0.35	0.82	2.94	9.29	0.10
SCV_250		Cane	18.4	2.9	3.9	62.9	0.38	1.10	3.91	6.41	0.18
SCV_329		Cane	10.0	2.2	5.2	65.8	0.36	0.63	6.73	8.99	0.16
SCV_364		Cane	12.4	3.0	1.0	68.8	0.28	0.82	5.62	7.99	0.04
SCV_365		Cane	15.6	2.9	3.0	66.4	0.43	0.96	3.61	7.01	0.13
SCV_366		Cane	14.4	2.0	2.1	70.1	0.29	0.91	3.15	6.96	0.04
SCV_368		Cane	15.4	3.0	3.0	66.3	0.43	0.92	3.58	7.26	0.13
SCV_369		Cane	18.1	4.6	4.6	62.3	0.36	1.17	4.58	6.22	0.17
SCV_388		Cane	18.5	3.9	3.9	63.1	0.37	1.18	3.71	6.26	0.17
SJT_001		Cane	12.9	3.7	5.1	58.4	0.38	0.78	7.29	11.29	0.17
SCV_044	White	Cane	15.8	2.3	5.9	62.5	0.41	1.81	4.53	6.50	0.25
SCV_216		Cane	11.2	2.9	1.8	68.7	0.30	0.81	4.90	9.33	0.07
SCV_232		Cane	15.5	3.0	4.8	61.7	0.39	0.86	5.67	7.85	0.20
SCV_245		Cane	14.8	3.5	0.9	67.2	0.39	0.71	2.27	10.17	0.05
SCV_250		Cane	17.3	2.6	3.7	64.4	0.40	1.66	3.42	6.31	0.16
SCV_329		Cane	12.7	3.5	1.4	67.1	0.31	0.72	4.43	9.79	0.06
SCV_360		Cane	15.7	3.0	2.1	66.8	0.37	1.13	3.43	7.43	0.10
SCV_364		Cane	12.1	2.9	1.6	69.9	0.29	0.92	5.59	6.63	0.04
SCV_365		Cane	18.0	2.2	2.9	66.2	0.60	1.34	3.64	4.94	0.20
SCV_368		Cane	18.6	1.9	2.8	66.4	0.80	1.57	3.47	4.21	0.24
SCV_369		Cane	18.9	3.3	4.0	61.4	0.44	1.39	3.68	6.77	0.15
SCV_375		Cane	17.7	3.1	3.5	64.0	0.34	0.74	3.34	7.18	0.13
SCV_388		Cane	19.4	2.7	3.3	63.4	0.40	1.54	3.10	5.88	0.16
SCV_394		Cane	18.9	1.6	1.1	66.1	0.90	2.22	3.73	5.32	0.08
SJT_001		Cane	15.0	3.7	2.7	62.6	0.34	1.06	6.03	8.47	0.09
SJT_009		Cane	13.9	3.5	3.1	61.9	0.38	0.87	7.35	8.93	0.07

Tab. S4. Composition of the analysed production waste and millefiori glass fragments unearth in Lisbon determined by LA-ICP-MS in weight percent of oxides up to iron oxide and in µg/g for all the remaining oxides. The chemical composition of red and clear glass presented in body glass of LCS_05 are highlighted. All the presented values were acquired through LA-ICP-MS analyses.

			Wt%											µg/g										
Sample	Color	Part	Na_2O	MgO	Al_2O_3	SiO_2	P_2O_5	Cl	K_2O	CaO	TiO_2	MnO	Fe_2O_3	CoO	NiO	CuO	ZnO	As_2O_3	SnO_2	SrO	ZrO_2	BaO	PbO	Bi
SCV_044	B	Cane	17.0	2.5	6.4	57.9	0.36	0.86	4.48	7.34	0.28	0.65	1.11	1430	291	226	75	2617	565	577	75	457	537	658
SCV_232		Body	10.4	3.0	2.0	64.5	0.26	0.68	4.53	9.68	0.07	0.38	1.31	4544	1514	1202	159	6268	6261	534	49	221	5308	5131
SCV_245		Cane	14.4	3.1	4.1	56.7	0.31	0.71	5.21	8.35	0.18	0.45	1.81	839	662	5906	96	2066	12489	496	126	312	2.32	809
SCV_250		Cane	14.3	3.5	1.5	65.7	0.31	0.89	2.18	10.02	0.06	0.06	0.81	1361	338	313	67	2773	444	700	24	134	532	456
SCV_329		Body	11.4	3.0	3.4	63.2	0.34	0.67	7.40	9.69	0.09	0.07	0.44	358	85	36	47	1119	<10	598	66	138	25	124
SCV_357		Body	18.2	3.0	4.0	59.8	0.31	1.09	3.45	7,42	0.14	0.40	0.95	1689	576	938	69	2695	2018	455	77	194	1819	1029
SCV_360		Body	15.9	2.9	2.3	64.9	0.33	0.99	4.20	6,92	0.11	0.29	0.82	456	148	202	59	500	772	733	55	456	521	409
SCV_360		Cane	15.3	3.0	2.2	64.5	0.29	0.97	3.86	7.50	0.11	0.37	1.08	3214	367	213	108	2194	482	656	47	200	466	343
SCV_364		Cane	11.9	2.9	1.0	67.2	0.27	0.81	5.64	6.83	0.05	0.02	1.23	5118	1460	2036	76	6556	138	489	24	75	258	3338
SCV_365		Body	17.1	1.9	3.4	65.3	0.42	1.07	3.73	4,42	0.23	0.70	1.21	606	204	190	113	720	1191	382	92	290	731	547
SCV_365		Cane	15.7	2.6	3.2	63.3	0.45	0.90	3.78	6.58	0.14	0.78	1.32	2639	799	350	171	2938	1304	542	70	445	904	1312
SCV_366		Cane	12.8	3.6	1.2	68.8	0.22	0.71	2.27	8.79	0.06	0.50	0.61	1038	332	53	62	1385	66	654	23	194	52	898
SCV_368		Body	17.0	1.9	3.4	65.3	0.42	1.09	3.80	4.42	0.23	0.71	1.21	603	202	145	111	717	1011	533	92	467	3125	1568
SCV_368		Cane	15.2	2.6	3.3	63.3	0.46	0.82	3.82	6.53	0.15	0.77	1.42	2991	910	461	197	3104	2514	385	70	290	610	524
SCV_369		Body	17.4	3.1	4.1	60.0	0.32	0.98	4.66	7.33	0.16	0.54	0.80	821	302	196	66	1347	483	480	77	238	6531	550
SCV_369		Cane	17.4	3.0	3.9	59.0	0.34	1.00	4.63	7.07	0.15	0.70	0.78	1242	387	5461	77	2108	1745	487	73	215	4623	425
SCV_375		Body	18.1	2.7	3.9	60.7	0.29	1.14	2.94	7.14	0.14	0.46	0.76	1021	354	460	61	1746	6168	413	77	208	1732	683
SCV_388		Body	18.4	2.8	3.8	61.0	0.36	1.16	3.24	6.70	0.18	0.53	0.99	1044	326	465	81	1527	1347	450	91	93	238	455
SCV_394		Body	17.0	1.8	0.9	67.3	0.37	1.26	3.88	5.81	0.06	0.29	0.93	1142	440	689	115	<10	231	206	35	94	220	n.d.
SJT_001		Body	12.4	3.5	4.3	57.7	0.41	0.67	7.17	11.26	0.14	0.59	1.20	627	82	55	55	1806	187	971	71	12	210	109
SJT_009		Body	13.7	3.6	3.4	59.2	0.32	0.64	7.30	9.50	0.08	0.49	0.87	1853	689	246	246	2887	745	737	46	<10	692	506
SCV_044	Cl	Body	20.2	2.8	6.8	55.8	0.33	1.14	3.99	6.88	0.32	0.55	1.06	148	49	50	74	250	363	634	284	443	386	88
SCV_046		Body	14.3	2.9	1.8	61.4	0.31	0.76	2.70	7.82	0.07	0.27	1.07	185	92	8833	63	544	29433	484	44	131	26083	88
SVC_235		Body	14.7	2.9	3.5	63.5	0.23	0.69	5.07	7.91	0.18	0.51	0.55	10	<10	12	39	<10	<10	652	126	384	10	<10
SVC_236		Body	14.0	3.1	5.4	59.0	0.25	0.70	6.77	8.83	0.23	0.56	0.93	73	41	310	71	127	130	477	145	374	207	26
SVC_245		Body	15.4	3.5	4.7	59.4	0.35	0.84	5.59	8.50	0.20	0.38	0.76	36	25	145	55	67	913	660	121	338	907	27
SVC_250		Body	15.4	3.0	5.6	62.0	0.31	0.95	3.77	7.31	0.21	0.39	0.96	12	11	16	53	20	<10	536	159	276	22	<10
SCV_272		Body	18.5	6.8	7.5	55.2	0.81	0.95	1.83	4.93	0.29	0.88	2.11	20	27	31	132	<10	<10	490	97	318	11	<10
SCV_275		Body	15.9	5.2	5.3	64.7	0.37	0.97	1.35	3.24	0.29	1.07	1.36	20	18	14	90	<10	<10	365	151	368	<10	<10
SCV_394		Cane	17.5	1.8	1.4	64.5	0.67	1.26	1.34	5.89	0.07	0.22	0.61	11	12	9500	121	<10	5295	240	33	148	10877	<10
SCV_232	G	Cane	10.8	3.1	2.2	65.1	0.25	0.83	4.88	10.21	0.07	0.40	0.94	163	69	2287	65	264	4236	551	54	231	3489	178
SCV_368	P	Cane	15.4	2.6	3.3	63.6	0.47	0.85	3.79	6.52	0.15	0.76	1.34	2998	847	473	189	3220	735	528	70	458	533	1489
SCV_044	R	Cane	15.6	2.9	7.1	55.4	0.55	0.82	4.69	6.88	0.34	0.41	2.83	97	46	4640	120	154	6743	475	311	354	6076	73
SCV_216		Cane	16.7	3.0	4.1	57.5	0.39	0.97	3.70	6.90	0.17	0.37	4.40	221	102	6025	84	432	4721	408	86	178	5639	136
SCV_232		Cane	10.2	2.9	2.1	62.1	0.26	0.74	4.61	9.48	0.07	0.35	4.70	179	83	14154	85	310	4584	511	50	210	3811	194
SCV_235		Cane	12.6	3.4	1.3	56.7	0.30	0.68	2.35	9.23	0.07	0.19	4.22	313	143	7413	62	907	34758	620	29	119	44990	192
SCV_245		Cane	14.5	3.2	5.4	57.3	0.38	0.80	5.26	8.36	0.22	0.52	0.98	121	74	7067	78	223	484	714	151	312	516	94

SCV_250		Cane	13.9	3.2	1.1	58.7	0.33	0.66	2.10	8.77	0.06	0.52	3.42	305	133	6537	82	782	37183	522	25	100	36597	102
SCV_275		Cane	12.8	3.2	1.1	56.6	0.31	0.64	2.02	8.37	0.05	0.68	2.61	399	105	7587	106	750	47149	560	23	137	60600	113
SCV_329		Cane	16.8	2.8	1.6	58.5	0.31	0.65	3.98	8.27	0.07	0.77	3.05	741	363	17776	107	1696	36317	510	38	200	37104	1039
SCV_357		Cane	12.6	3.5	4.5	57.7	0.39	0.98	3.40	7.47	0.15	0.22	3.42	110	66	9859	66	195	1453	444	79	159	1297	92
SCV_360		Cane	10.3	2.8	2.9	61.2	0.35	0.78	3.66	6.57	0.13	0.37	3.12	81	85	21440	130	188	3231	615	55	212	2170	135
SCV_364		Cane	11.5	2.8	1.2	63.9	0.29	0.74	3.36	6.63	0.05	0.02	4.62	20	29	24732	32	52	1697	466	466	76	2016	11
SCV_369		Cane	15.0	3.4	4.2	57.6	0.43	0.91	4.07	7.89	0.17	0.22	1.62	27	30	12749	64	70	1466	417	79	149	17504	22
SCV_375		Cane	16.2	3.3	4.0	55.2	0.38	0.99	3.37	7.08	0.15	0.20	2.85	58	47	9785	66	113	22619	423	75	148	30072	48
SCV_388		Cane	16.0	3.3	4.4	58.2	0.42	0.93	3.12	7.17	0.18	0.37	3.70	178	121	7758	76	359	3930	445	86	197	4052	135
SCV_394		Cane	14.8	3.5	2.0	64.4	0.50	0.85	3.24	6.39	0.10	0.37	2.36	57	87	15183	2158	69	2255	286	52	212	3014	<10
SJT_001		Cane	13.9	3.2	3.9	57.7	0.39	0.69	6.44	8.80	0.11	0.44	2.71	68	31	13316	69	217	629	582	66	253	691	17
SJT_009		Cane	13.5	3.5	3.4	57.3	0.34	0.59	7.15	9.13	0.08	0.46	3.58	59	28	6488	50	97	714	692	46	267	651	36
SCV_216	T	Body	17.7	2.7	3.7	60.4	0.37	1.60	3.75	6.15	0.17	0.20	1.00	36	55	24845	62	92	682	444	85	150	973	39
SCV_250		Cane	14.0	3.3	2.3	61.4	0.33	0.77	2.75	8.70	0.10	0.45	1.55	229	91	1916	76	530	20708	549	64	147	18647	72
SCV_329		Cane	9.0	1.9	4.7	59.5	0.32	0.57	6.09	8.13	0.14	0.17	0.68	38	114	79704	113	207	3028	508	96	267	2682	20
SCV_364		Cane	12.2	2.9	1.0	67.3	0.27	0.81	5.50	6.80	0.04	0.02	0.52	5153	1483	1185	77	6805	123	490	24	75	276	3197
SCV_365		Cane	15.1	2.8	2.9	64.2	0.42	0.93	3.49	6.78	0.13	0.77	0.91	30	33	12617	115	50	887	573	61	279	905	25
SCV_366		Cane	10.6	1.6	0.7	55.4	0.23	0.72	2.43	5.52	0.03	0.40	0.01	73	60	29622	51	119	11.93	588	15	110	88852	24
SCV_368		Cane	14.8	2.9	2.9	63.7	0.41	0.88	3.44	6.97	0.12	0.68	0.94	33	41	19306	126	66	1513	592	58	274	1054	32
SCV_369		Cane	16.6	2.4	4.2	57.2	0.33	1.08	4.20	5.71	0.15	0.04	0.71	<10	74	71156	53	103	592	319	79	105	1574	15
SCV_388		Cane	17.6	2.6	3.7	60.1	0.35	1.12	3.53	5.96	0.17	0.22	0.92	46	84	32668	78	148	1119	424	83	145	1689	60
SJT_001		Cane	12.6	3.6	5.0	56.9	0.37	0.76	7.10	11.0	0.16	0.57	1.39	777	70	480	22	1942	212	915	87	251	446	79
SCV_044	W	Cane	10.5	1.6	4.0	41.5	0.27	1.10	2.99	4.33	0.17	0.17	0.67	23	39	965	75	55	13.2	354	199	181	19.59	60
SCV_216		Cane	10.9	1.6	2.3	40.4	0.25	1.04	2.15	3.96	0.10	0.14	0.47	28	47	754	52	92	15.8	240	58	137	20.66	27
SCV_232		Cane	8.0	2.1	1.3	49.1	0.21	0.58	3.51	6.68	0.05	0.27	0.69	247	132	601	78	678	16.4	359	35	252	10.79	395
SCV_245		Cane	12.5	2.4	3.9	49.7	0.31	0.69	4.56	6.32	0.16	0.26	0.66	46	41	1309	74	487	4.3	601	101	88	13.89	75
SCV_250		Cane	12.4	2.9	0.7	56.4	0.33	0.60	1.91	8.54	0.04	0.78	0.67	75	51	1361	54	242	6.6	484	18	98	7.73	34
SCV_329		Cane	9.7	2.6	1.0	51.1	0.24	0.55	3.37	7.45	0.04	0.59	0.60	82	48	224	51	319	10.1	513	24	109	12.40	141
SCV_360		Cane	10.7	2.1	1.4	45.7	0.26	0.78	2.35	5.08	0.07	0.21	0.52	14	38	115	57	248	15.0	491	33	116	15.57	10
SCV_364		Cane	8.7	2.1	0.6	50.1	0.21	0.65	3.98	4.72	0.03	0.09	0.33	63	59	372	21	84	12.1	349	16	73	16.12	59
SCV_365		Cane	13.2	1.6	2.1	48.4	0.44	0.98	2.66	3.61	0.15	0.35	0.90	24	46	931	75	37	15.6	279	63	149	9.82	19
SCV_368		Cane	10.4	1.1	1.5	37.2	0.45	0.88	1.94	2.36	0.13	0.16	0.75	22	73	1697	72	39	30.6	177	56	97	12.10	17
SCV_369		Cane	12.4	2.2	2.6	40.2	0.29	0.91	2.41	4.43	0.10	0.07	0.50	12	43	22723	41	47	13.5	249	52	77	18.02	14
SCV_375		Cane	13.4	2.3	2.7	48.4	0.26	0.56	2.53	5.43	0.10	0.23	0.49	31	42	3436	48	52	12.3	343	54	117	10.83	25
SCV_388		Cane	11.9	1.7	2.1	39.0	0.25	0.95	1.91	3.62	0.10	0.22	0.44	33	53	7089	61	71	18.3	250	58	97	18.72	30
SCV_394		Cane	14.9	1.3	0.9	52.1	0.71	1.75	2.93	4.19	0.06	0.13	0.47	<10	22	2259	99	37	6.8	168	27	63	13.46	74
SJT_001		Cane	11.5	2.8	2.1	47.9	0.26	0.81	4.61	6.47	0.06	0.22	0.58	42	30	4406	36	190	7.77	455	37	143	14.37	17
SJT_009		Cane	10.3	2.6	2.3	45.9	0.28	0.65	5.45	6.62	0.05	0.23	0.57	52	47	113	47	221	12.12	481	32	144	12.70	43

B = Blue; Cl= Clear; G = Green; P = Purple; R= Red; T= Turquoise; W= White;

Tab. S2: (Suplementary material): Presentation of the glass composition for the glass materia

	oxyde	Na2O	MgO	Al2O3
N610	av. % oxide	13,2%	0,081%	2,02%
	av. ppm element	98 132	486	10 704
	RSD	2,0%	0,5%	4,7%
N612	av. % oxide	13,5%	0,011%	2,07%
	av. ppm element	100 471	64	10 941
	RSD	2,2%	0,9%	3,4%
CORNA	av. % oxide	13,9%	2,55%	0,92%
	av. ppm element	102 902	15 374	4 856
	RSD	2,5%	0,9%	4,1%
CORNB	av. % oxide	16,8%	1,02%	4,37%
	av. ppm element	124 546	6 163	23 103
	RSD	2,4%	1,1%	3,9%
CORND	av. % oxide	1,31%	3,98%	5,29%
	av. ppm element	9 685	23 992	27 983
	RSD	2,6%	1,7%	3,2%
CORNC	av. % oxide	1,08%	2,65%	0,78%
	av. ppm element	8 031	15 952	4 144
All the standards	RSD	4,0%	2,9%	3,8%
	average RSD	2,6%	1,3%	3,8%
	max RSD	4,0%	2,9%	4,7%

ıl used for the calibration of LA-ICP-MS equipment (N610, N612, CORNA, CORNB, COF

SiO2	P2O5	Cl	K2O	CaO
70,4%	0,098%	0,076%	0,053%	11,5%
329 046	429	759	443	81 914
0,3%	2,2%	4,7%	2,3%	0,8%
72,4%	0,015%	0,059%		11,6%
338 623	64	590		83 124
0,5%	5,1%	7,1%		1,1%
67,0%	0,11%	0,14%	2,82%	5,61%
313 134	493	1 396	23 451	40 061
0,3%	2,1%	4,2%	1,1%	0,7%
62,4%	0,80%	0,21%	1,01%	8,64%
291 679	3 511	2 057	8 408	61 771
0,3%	2,4%	1,9%	1,7%	1,0%
55,4%	4,04%	0,22%	11,2%	14,9%
258 795	17 613	2 231	92 958	106 579
0,1%	2,4%	2,1%	1,5%	1,3%
35,7%	0,12%	0,13%	2,80%	6,68%
166 966	513	1 330	23 230	47 723
1,2%	4,2%	5,4%	0,8%	2,3%
0,4%	3,1%	4,2%	1,5%	1,2%
1,2%	5,1%	7,1%	2,3%	2,3%

RND and CORNC). The composition is presented in average (wt% for oxides and µg

TiO2	MnO	Fe2O3	CuO	Sb2O3
0,073%	0,060%	0,068%	0,054%	0,050%
437	467	478	433	414
3,0%	2,7%	1,8%	3,8%	1,6%
0,0070%	0,0052%	0,0070%	0,0044%	0,0041%
42	40	49	35	34
4,0%	2,5%	4,0%	3,3%	1,2%
0,74%	1,02%	1,12%	1,16%	1,66%
4 437	7 905	7 820	9 285	13 830
3,0%	2,9%	2,9%	3,7%	2,1%
0,10%	0,24%	0,34%	2,63%	0,43%
607	1 896	2 403	20 980	3 578
2,7%	2,9%	2,8%	3,9%	3,0%
0,38%	0,56%	0,51%	0,36%	0,90%
2 251	4 306	3 558	2 858	7 540
4,2%	2,4%	2,6%	3,3%	1,8%
0,74%	0,00%	0,31%	1,19%	0,00%
4 458	10	2 169	9 510	3
4,2%	1,0%	1,5%	2,5%	32,9%
3,5%	2,4%	2,6%	3,4%	7,1%
4,2%	2,9%	4,0%	3,9%	32,9%

µg for the elements) as well as the relative standart deviations (RSD) for each referenced glass.

PbO	Li2O	B2O3	V2O5	Cr2O3	CoO
0,039%	0,10%	0,11%	0,079%	0,060%	0,053%
364	473	353	445	408	418
4,9%	5,1%	0,9%	2,4%	2,0%	2,3%
0,0034%	0,0089%	0,011%	0,0069%	0,0052%	0,0044%
31	41,3	35,0	38,7	35,5	34,9
2,8%	5,6%	0,5%	2,1%	4,1%	2,0%
0,062%	0,011%	0,21%	0,0065%	0,0034%	0,17%
572	49,1	650	36,3	23,1	1 345
3,2%	6,1%	0,9%	2,5%	8,8%	2,1%
0,42%	0,0024%	0,031%	0,034%	0,0090%	0,044%
3 942	11,0	96,3	191	61,4	346
5,3%	6,8%	1,2%	2,3%	2,8%	2,3%
0,20%	0,0061%	0,11%	0,018%	0,0028%	0,019%
1 859	28,1	331	98,5	19,0	148
4,5%	6,6%	0,9%	2,2%	6,2%	1,7%
36,3%	0,010%	0,23%	0,0069%		0,18%
336 854	46,3	711	38,5		1 417
2,1%	6,8%	2,0%	4,0%		0,7%
3,8%	6,2%	1,1%	2,6%	4,8%	1,8%
5,3%	6,8%	2,0%	4,0%	8,8%	2,3%

NiO	ZnO	GaO	As2O3	Se	Rb2O
0,057%	0,057%	0,054%	0,042%	0,041%	0,048%
447	460	442	320	406	437
3,8%	2,6%	4,2%	2,7%	9,7%	1,3%
0,0047%	0,0045%	0,0044%	0,0043%		0,0035%
36,6	36,3	35,8	32,6		32,0
3,0%	2,1%	3,2%	3,4%		1,2%
0,022%	0,054%		0,0036%		0,0095%
176	437	*0,89*	27,0		86,8
2,8%	0,6%		4,6%		1,0%
0,092%	0,22%	0,0003%	0,0026%		0,0013%
721	1 752	2,26	20,0		11,5
2,2%	1,5%	2,7%	3,2%		1,3%
0,047%	0,11%	0,0003%	0,035%		0,0047%
368	859	2,51	265		42,6
3,2%	0,9%	4,0%	3,4%		1,2%
0,020%	0,062%				0,0092%
156	497	*0,47*	*3,02*		84,2
1,4%	1,8%				0,6%
2,7%	1,6%	3,5%	3,5%	9,7%	1,1%
3,8%	2,6%	4,2%	4,6%	9,7%	1,3%

SrO	Y2O3	ZrO2	Nb2O3	MoO	Ag
0,059%	0,058%	0,060%	0,053%	0,044%	0,025%
500	453	443	422	379	250
1,5%	0,7%	1,2%	2,0%	0,7%	6,7%
0,0091%	0,0049%	0,0052%	0,0045%	0,0038%	0,0020%
77,2	38,3	38,1	35,5	32,7	20,2
1,3%	0,7%	1,7%	1,6%	0,4%	2,3%
0,10%		0,0053%			
881	*0,54*	39	*0,52*	*2,29*	*15,1*
1,2%		1,9%			
0,018%		0,0238%			
149	*0,46*	177	*0,15*	*1,28*	*63,1*
1,3%		1,1%			
0,057%		0,0122%			
479	*0,46*	90	*0,48*	*2,51*	
0,8%		1,4%			
0,29%		0,0050%			
2 416	*8,01*	37	*0,48*	*2,86*	*16,6*
0,9%		4,0%			
1,2%	0,7%	1,9%	1,8%	0,6%	4,5%
1,5%	0,7%	4,0%	2,0%	0,7%	6,7%

Cd	In	SnO2	Cs2O	BaO	La2O3
0,040%	0,045%	0,051%	0,039%	0,048%	0,054%
403	446	401	364	426	456
1,8%	4,0%	3,2%	3,0%	3,2%	2,6%
0,0042%	0,0037%	0,0043%	0,0043%	0,0040%	0,0045%
41,6	36,7	33,6	40,7	35,7	38,2
1,7%	3,2%	2,9%	2,3%	0,8%	2,3%
		0,17%		0,45%	
0,50		1 331	*0,26*	4 065	*0,32*
		3,2%		1,3%	
		0,024%		0,077%	
1,14		186		688	*0,20*
		4,2%		2,3%	
		0,082%		0,29%	
0,31		647		2 580	*0,49*
		3,3%		1,1%	
		0,19%		10,5%	
0,94		1 487		93 913	*0,66*
		1,3%		1,1%	
1,8%	3,6%	3,0%	2,6%	1,6%	2,5%
1,8%	4,0%	4,2%	3,0%	3,2%	2,6%

CeO2	PrO2	Nd2O3	Sm2O3	Eu2O3	Gd2O3	Tb2O3
0,055%	0,054%	0,052%	0,054%	0,055%	0,051%	0,053%
448	438	443	466	477	439	459
1,8%	2,5%	4,0%	5,2%	4,9%	6,7%	5,3%
0,0047%	0,0045%	0,0041%	0,0043%	0,0042%	0,0040%	0,0044%
38,4	36,8	35,0	37,1	36,7	35,1	37,9
1,6%	1,9%	2,3%	2,9%	3,3%	3,7%	3,8%
0,24	*0,03*	*0,12*				
0,16	*0,02*	*0,07*				
0,27	*0,02*	*0,09*				
0,15	*0,03*					
1,7%	2,2%	3,2%	4,1%	4,1%	5,2%	4,6%
1,8%	2,5%	4,0%	5,2%	4,9%	6,7%	5,3%

Dy2O3	Ho2O3	Er2O3	Tm2O3	Yb2O3	Lu2O3	HfO2	Ta2O3
0,051%	0,053%	0,051%	0,050%	0,055%	0,051%	0,051%	0,044%
442	467	442	436	481	452	433	391
5,1%	5,6%	5,5%	5,7%	6,0%	5,9%	5,0%	5,4%
0,0040%	0,0044%	0,0041%	0,0041%	0,0044%	0,0042%	0,0042%	0,0036%
34,6	38,5	35,9	36,2	39,0	37,0	35,5	31,5
3,7%	3,8%	3,4%	3,8%	4,1%	4,0%	3,2%	3,4%
						0,0001%	
						0,93	*0,10*
						3,9%	
						0,0005%	
						3,94	*0,07*
						4,7%	
						0,0002%	
						2,04	*0,17*
						3,9%	
						0,0001%	
						0,98	
						3,0%	
4,4%	4,7%	4,5%	4,7%	5,1%	4,9%	3,9%	4,4%
5,1%	5,6%	5,5%	5,7%	6,0%	5,9%	5,0%	5,4%

WO	Pt	Au	Bi	ThO2	UO2
0,037%	0,000%	0,002%	0,037%	0,052%	0,054%
336	3,28	22,8	373	454	472
6,4%	8,1%	5,2%	6,6%	2,8%	4,4%
0,0030%	0,0002%	0,0005%	0,0030%	0,0042%	0,0042%
27,2	2,42	4,54	29,9	37,3	37,3
3,8%	2,5%	2,8%	3,9%	1,7%	2,8%
	0,0004%		0,0009%		
	3,68	*0,11*	8,61	*0,28*	*0,19*
	6,2%		4,8%		
	0,0001%		0,0040%		
	1,24		40,0	*0,80*	*0,22*
	8,1%		6,6%		
	0,0001%		0,0011%		
	0,75		11,4	*0,64*	*0,16*
	4,7%		5,9%		
	0,0006%		0,0051%		
	6,08		51,0	*0,19*	*0,06*
	4,3%		3,6%		
5,1%	5,6%	4,0%	5,2%	2,3%	3,6%
6,4%	8,1%	5,2%	6,6%	2,8%	4,4%